SUPPLEMENTARY MATERIAL

New dibenzocyclooctadiene lignans from *Kadsura induta* with their anti-inflammatory activity

Bui Huu Tai[a,b], Pham Hai Yen[a], Nguyen Huy Hoang[a], Phan Thi Thanh Huong[a], Nguyen Viet Dung[a], Bui Van Thanh[c], Nguyen The Cuong[c], Ngo Anh Bang[a], Nguyen Xuan Nhiem[a,b], and Phan Van Kiem[a,b,*]

[a)]*Institute of Marine Biochemistry, Vietnam Academy of Science and Technology (VAST), 18 Hoang Quoc Viet, Cau Giay, Hanoi, Vietnam.*

[b)]*Graduate University of Science and Technology, VAST, 18 Hoang Quoc Viet, Cau Giay, Hanoi, Vietnam.*

[c)]*Institute of Ecology and Biological Resources, VAST, 18 Hoang Quoc Viet, Cau Giay, Hanoi, Vietnam.*

Corresponding author:

Phan Van Kiem, Prof. Ph.D. E-mail: phankiem@yahoo.com

Institute of Marine Biochemistry, Vietnam Academy of Science and Technology

18-Hoang Quoc Viet, Cau Giay, Hanoi, Vietnam

Content

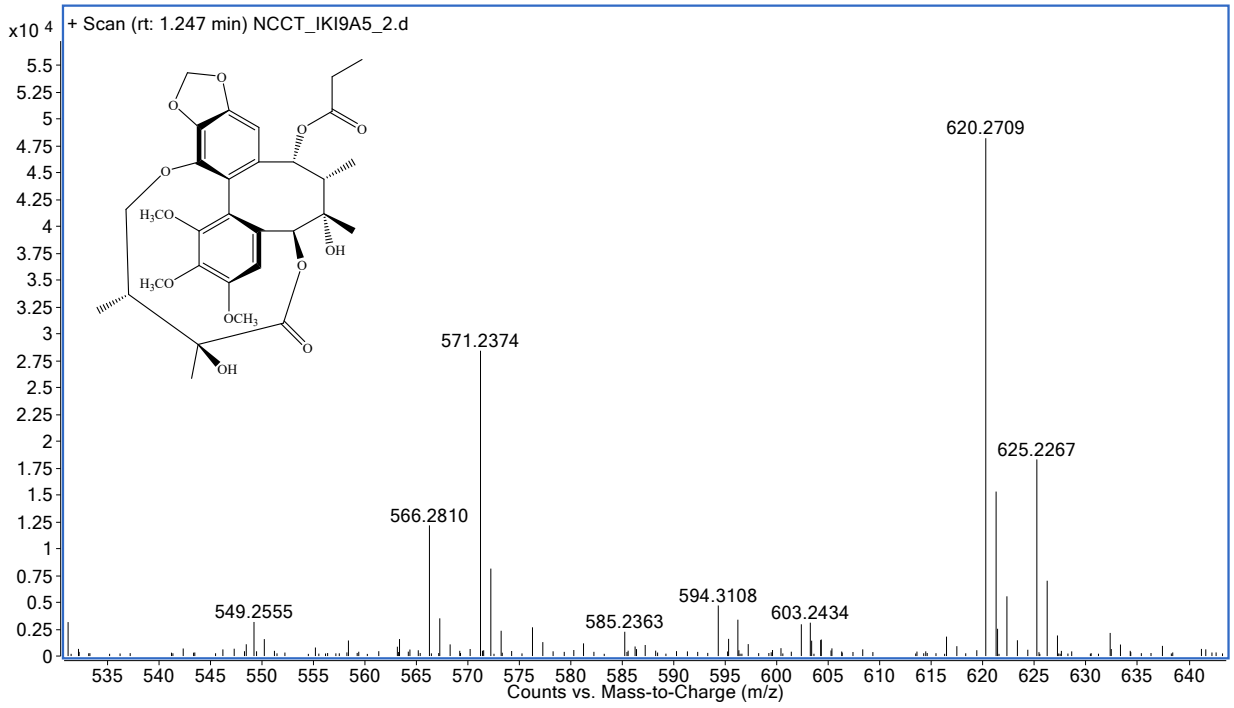

Figure S1. HR-ESI-MS of compound **1**

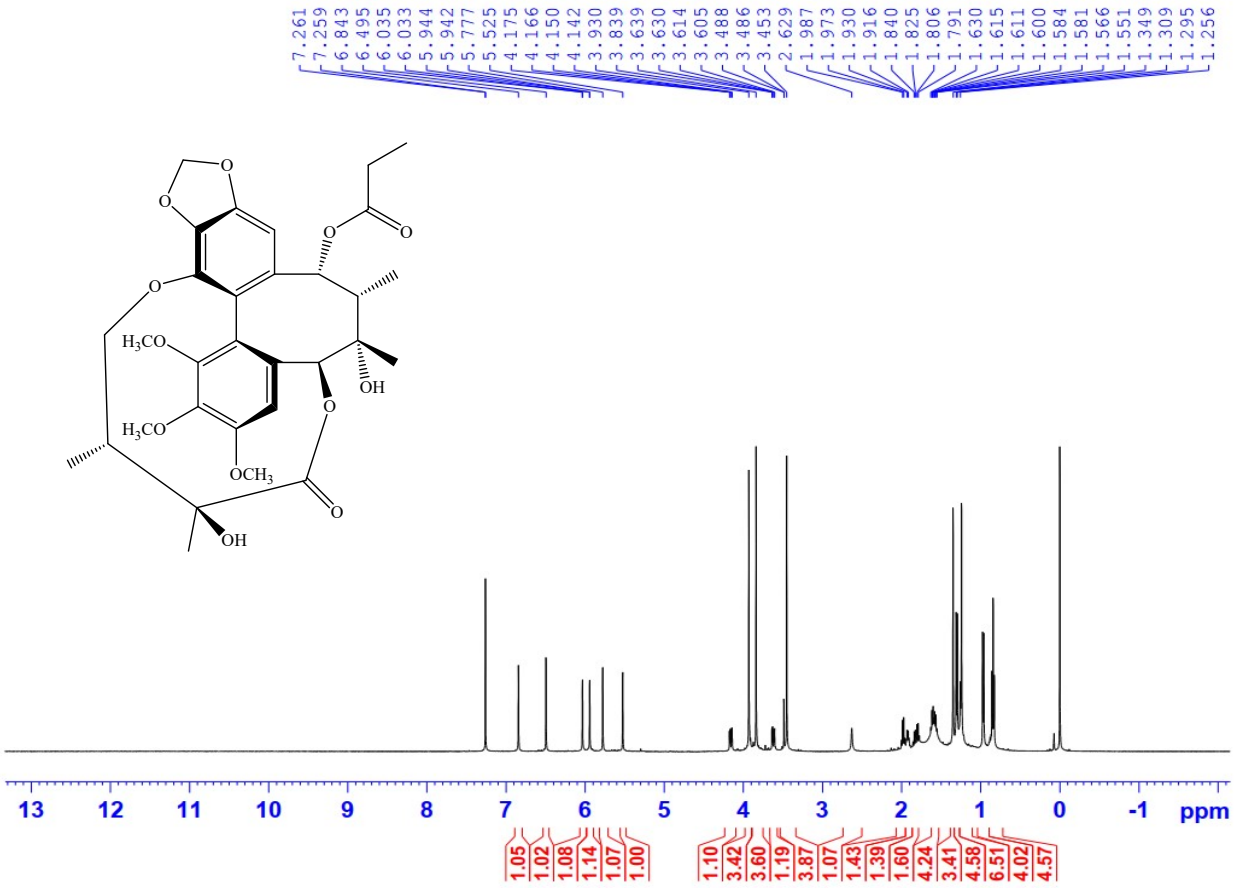

Figure S2. ^{1}H-NMR spectrum of compound **1** in $CDCl_3$

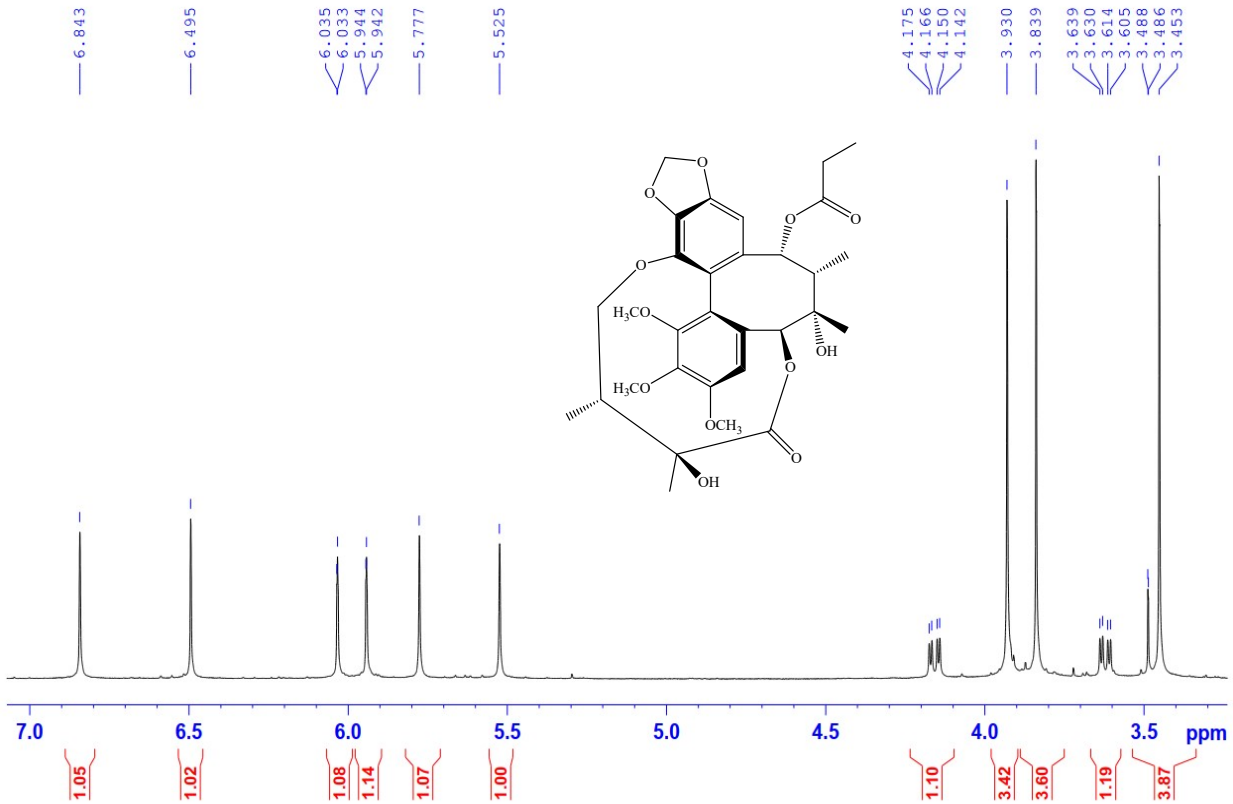

Figure S3. Expanded ^{1}H-NMR spectrum of compound **1**

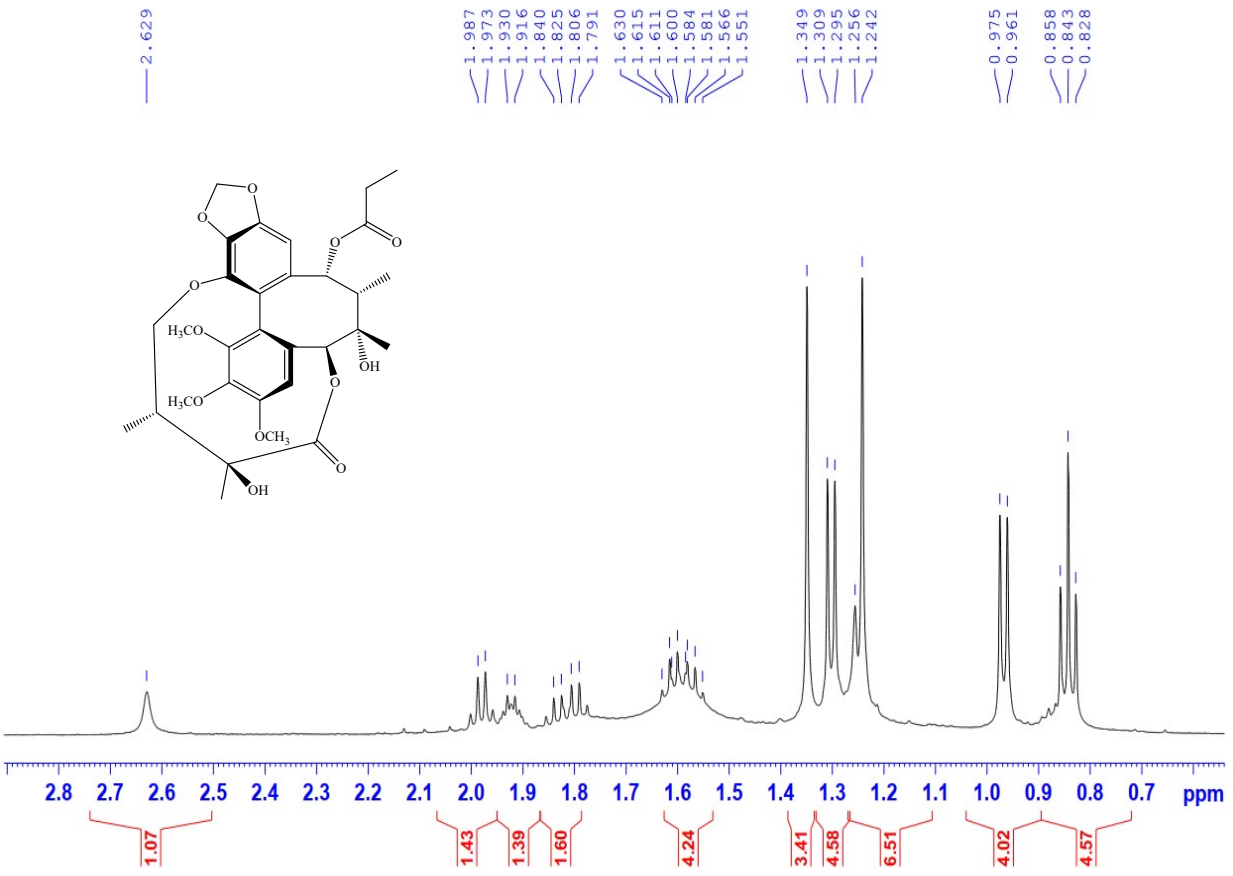

Figure S4. Expanded ^{1}H-NMR spectrum of compound **1**

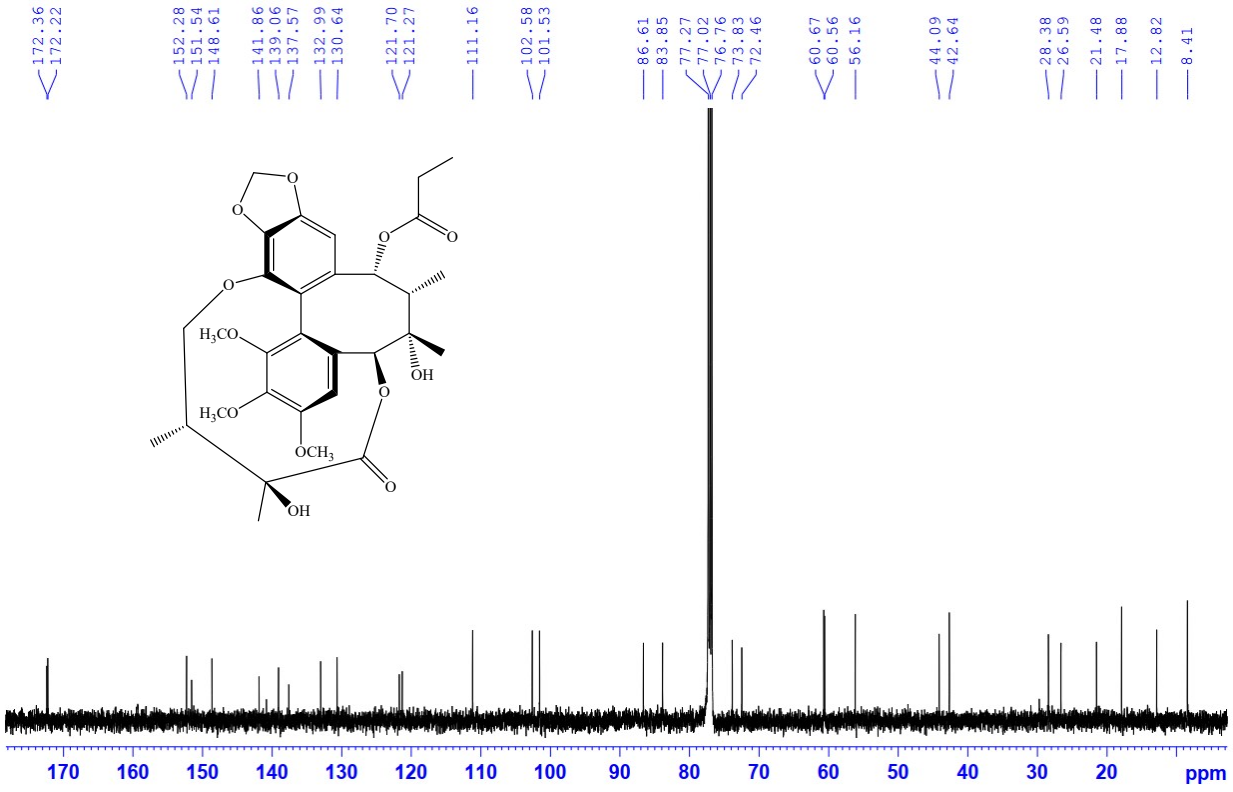

Figure S5. ^{13}C-NMR spectrum of compound **1** in $CDCl_3$

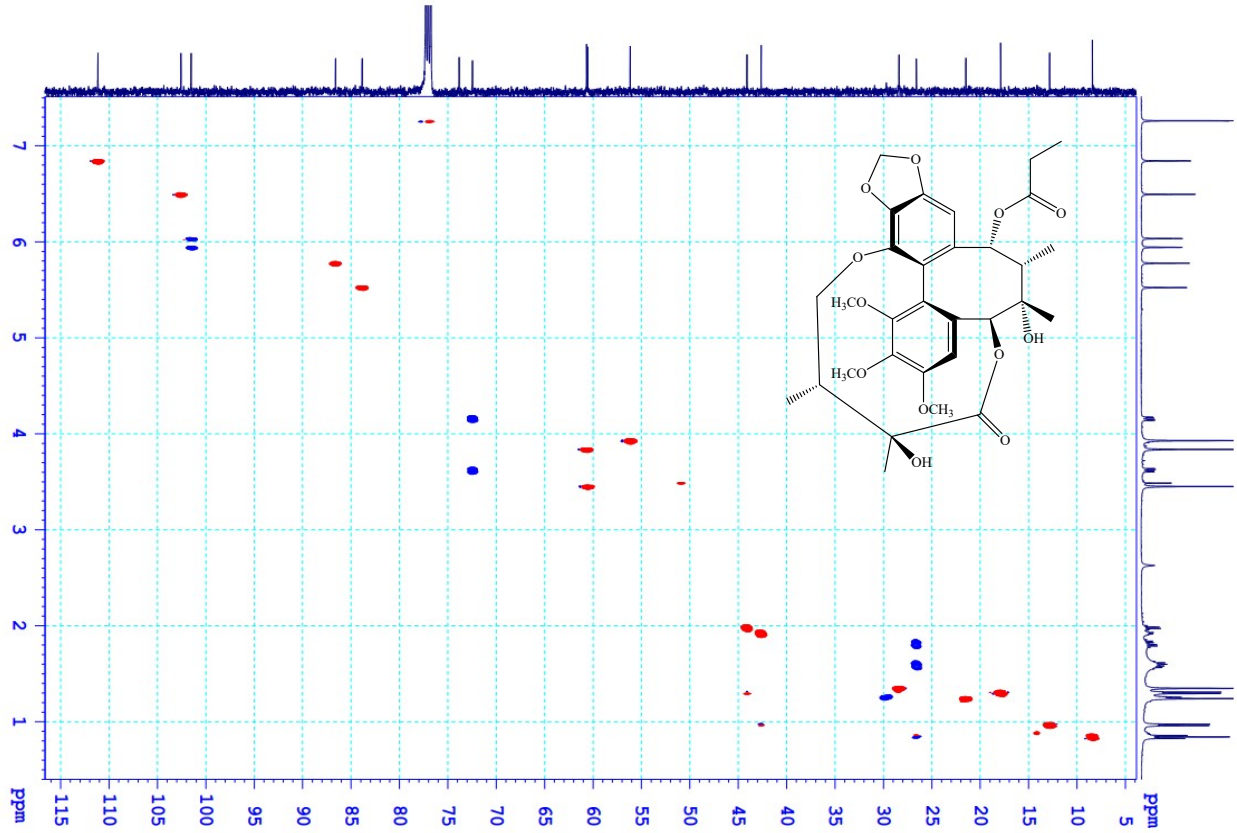

Figure S6. HSQC spectrum of compound **1**

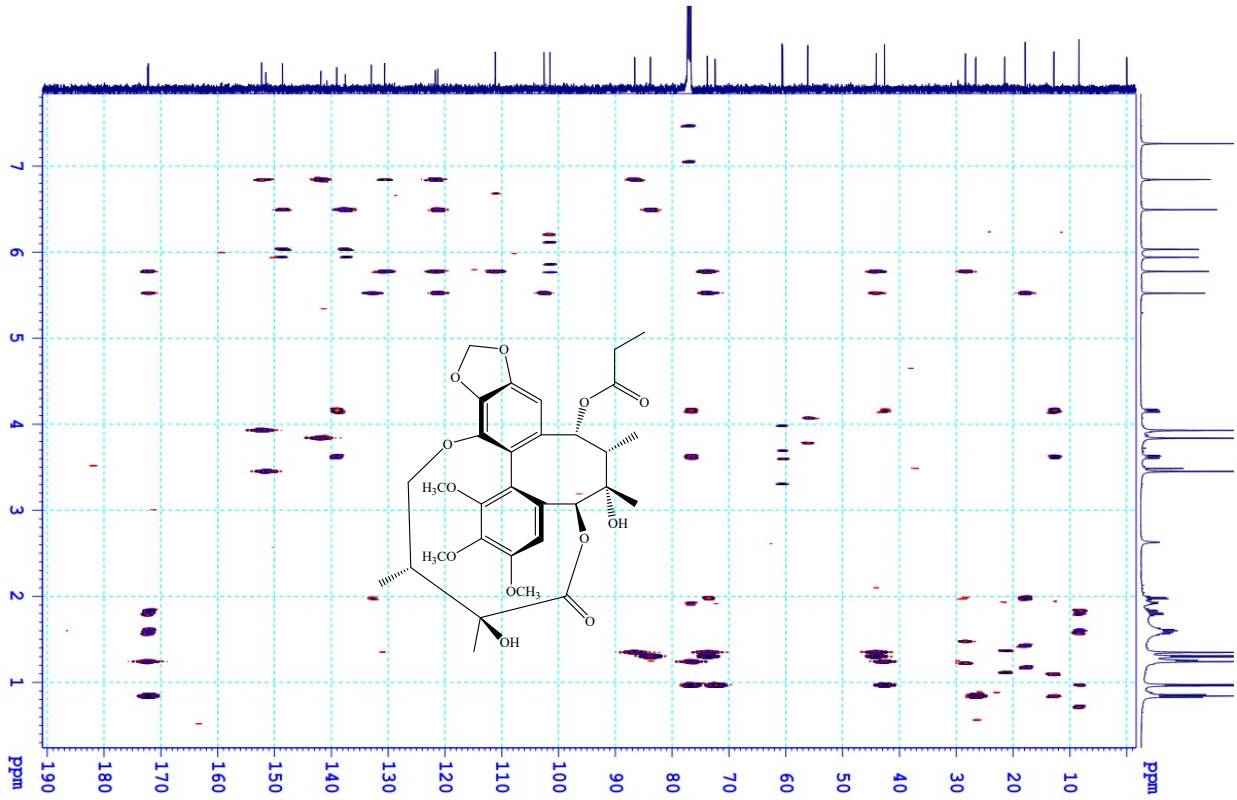

Figure S7. HMBC spectrum of compound **1**

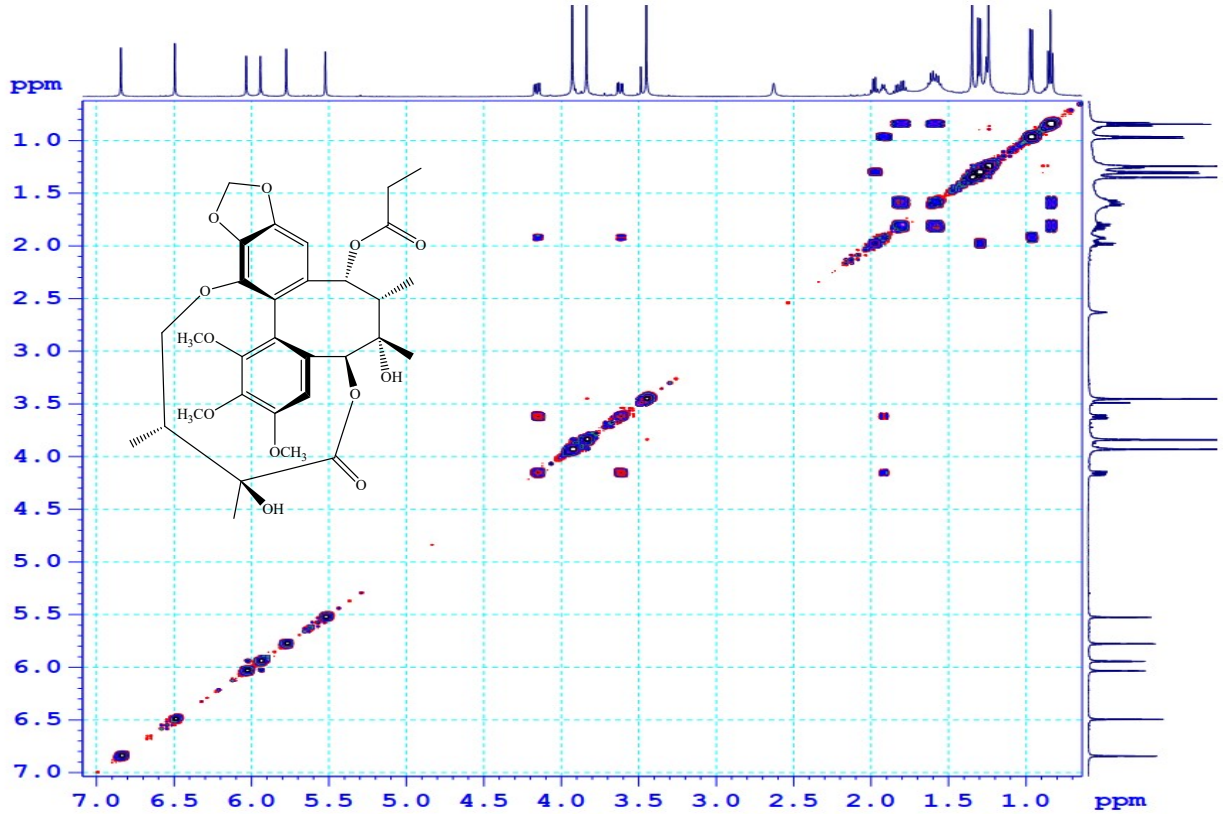

Figure S8. COSY spectrum of compound **1**

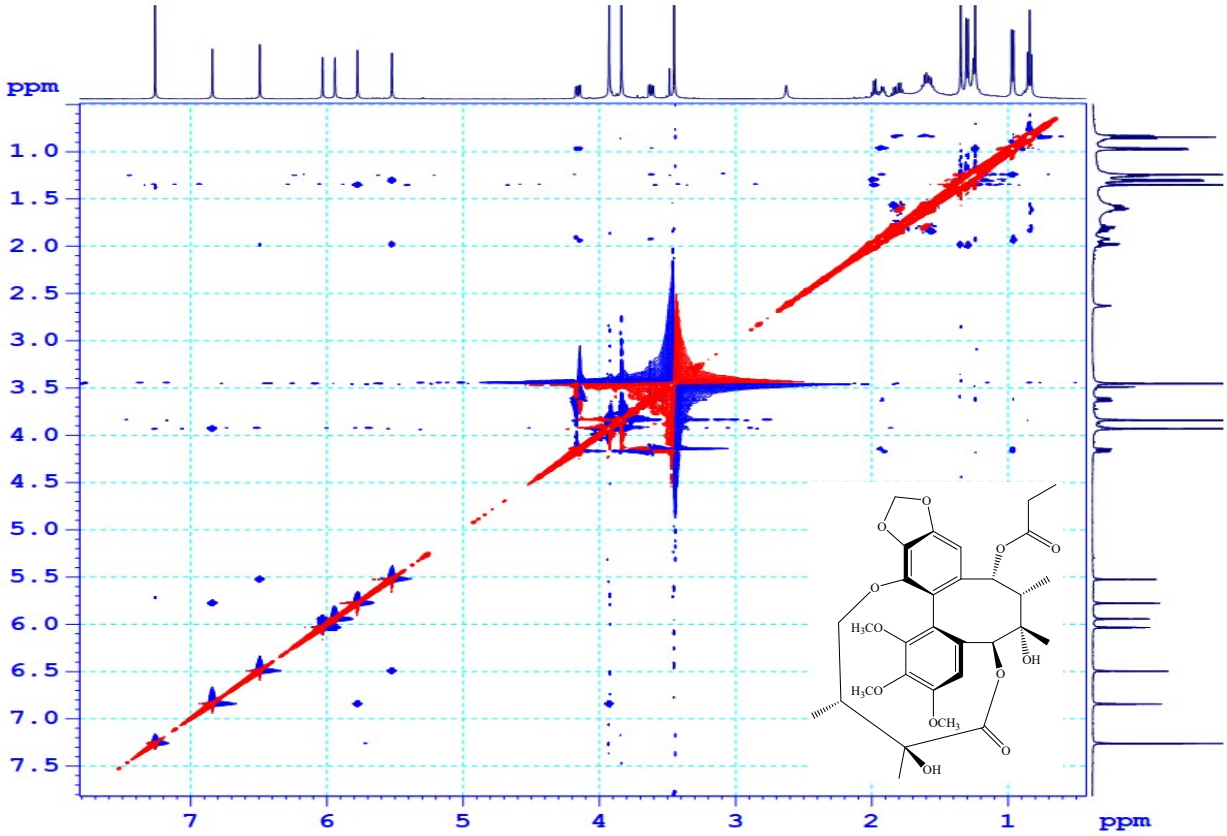

Figure S9. NOESY spectrum of compound **1**

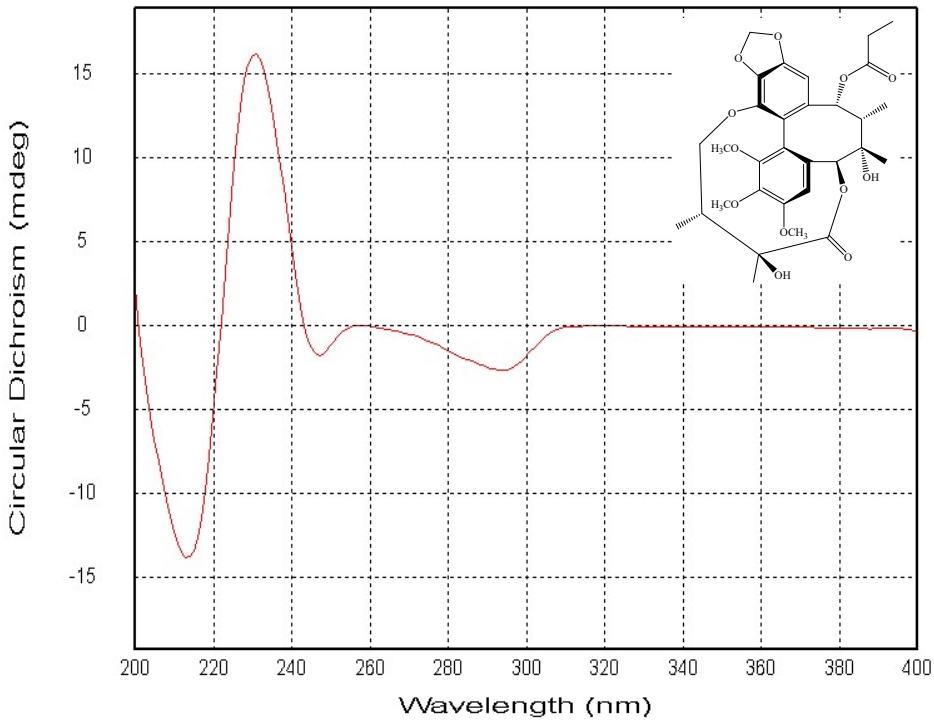

Figure S10. ECD spectrum of compound **1**

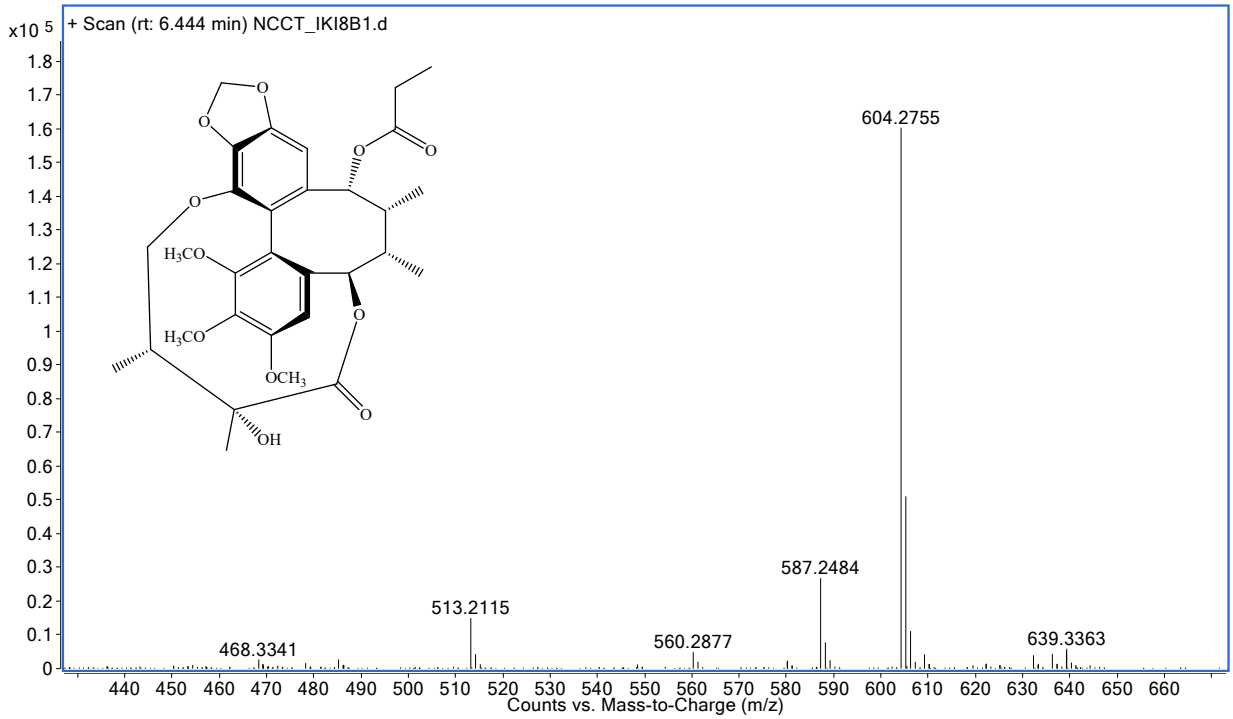

Figure S11. HR-ESI-MS of compound **2**

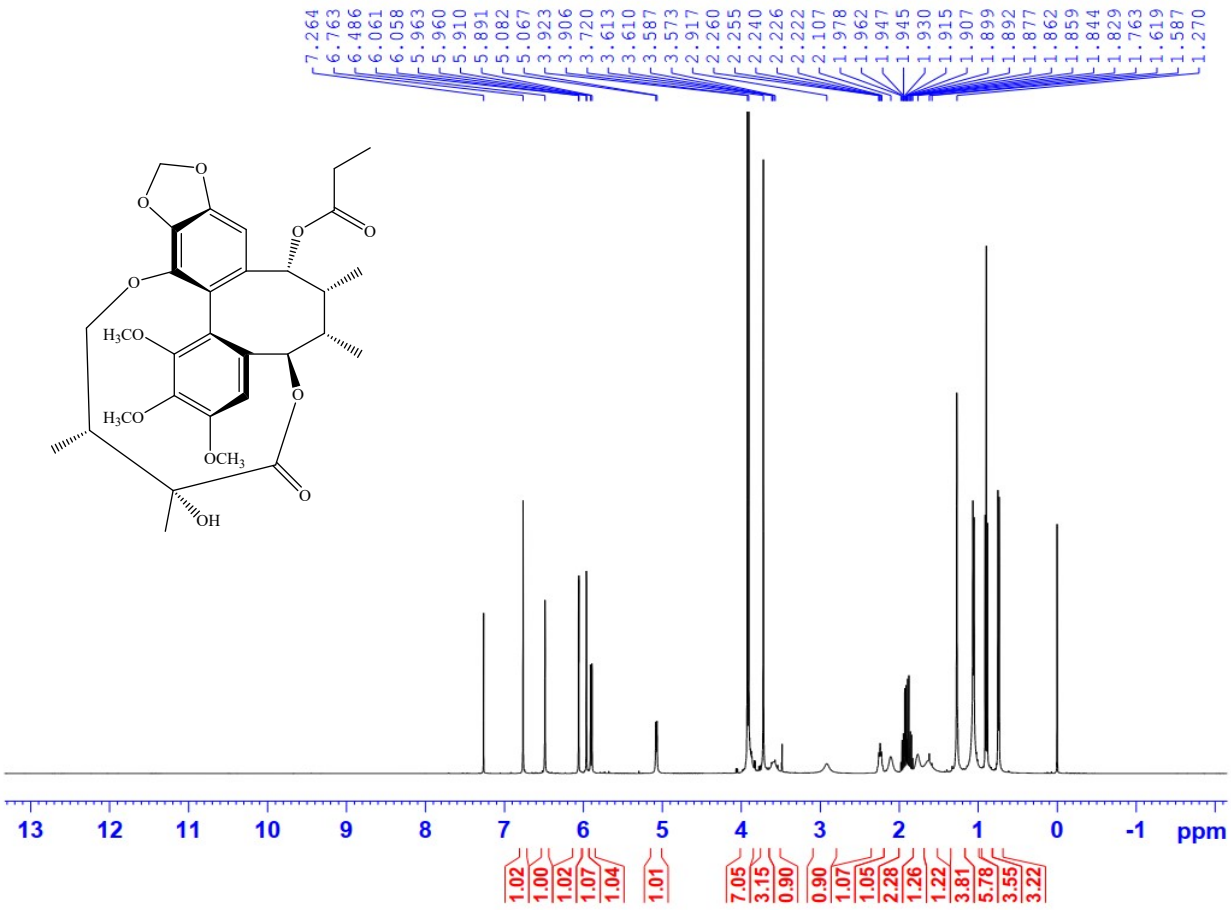

Figure S12. ^{1}H-NMR spectrum of compound **2** in $CDCl_3$

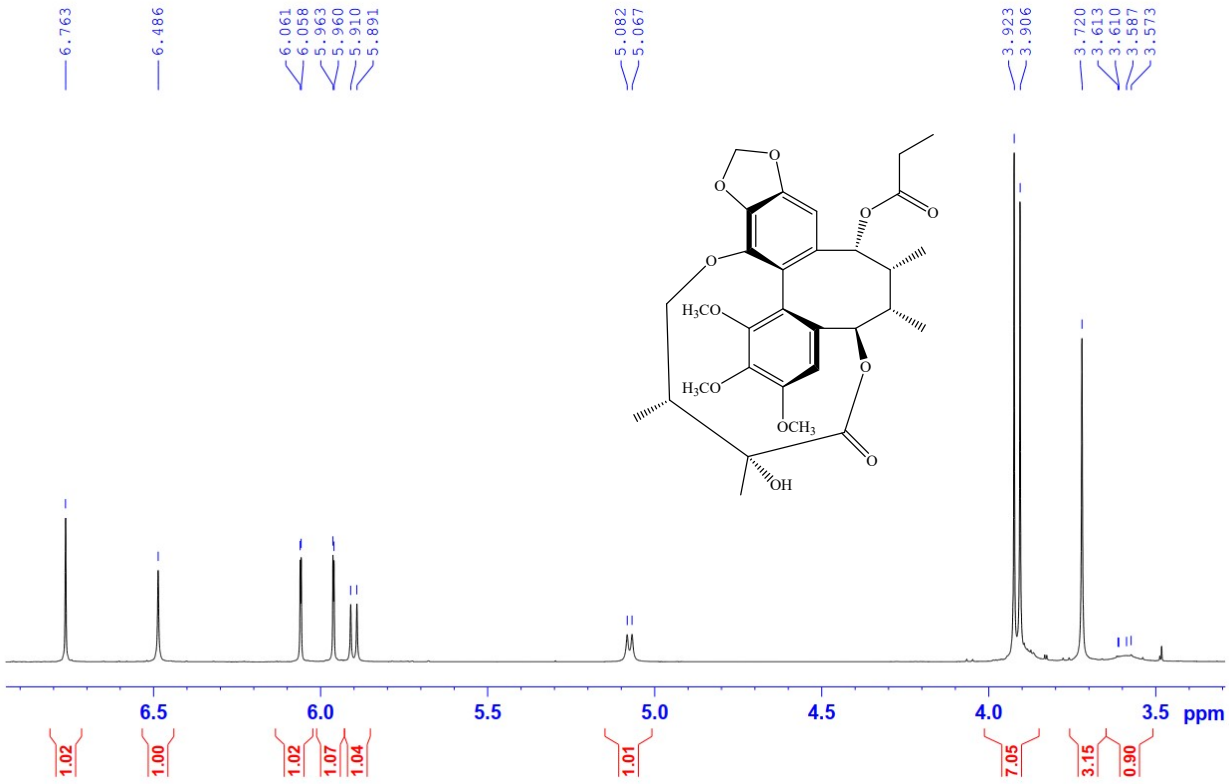

Figure S13. Expanded [1]H-NMR spectrum of compound **2**

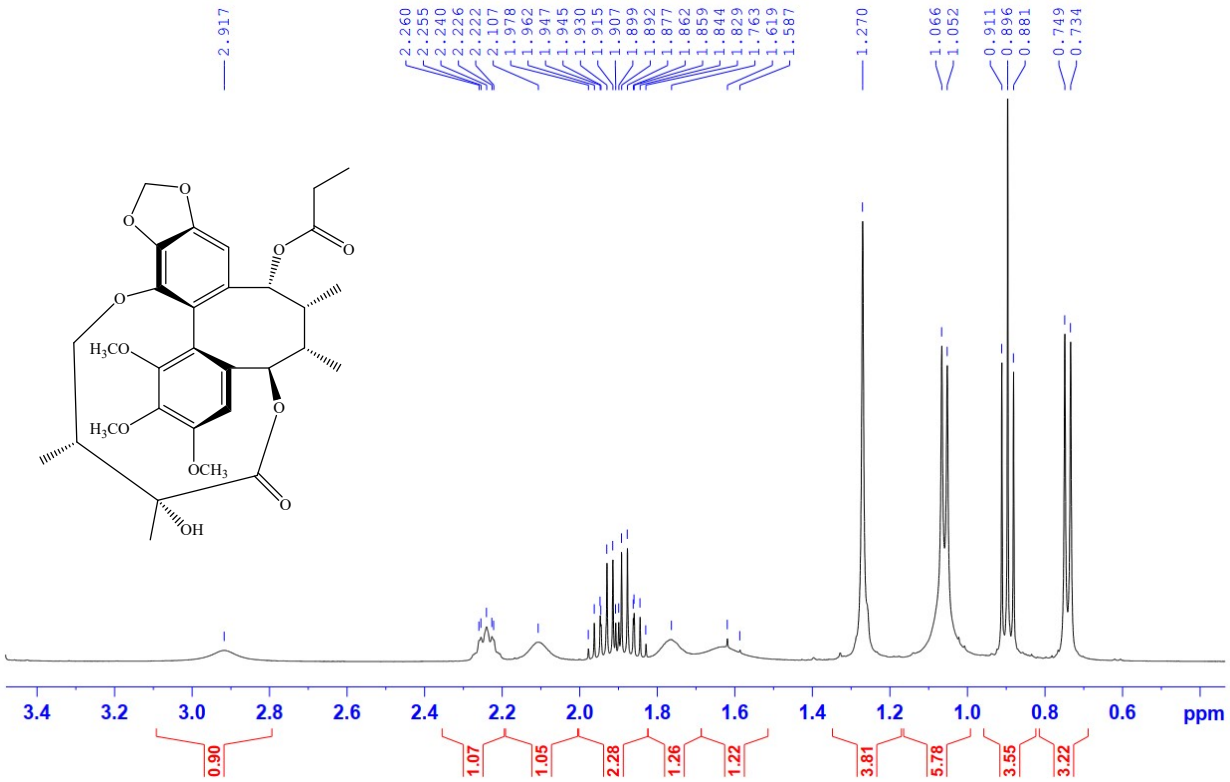

Figure S14. Expanded [1]H-NMR spectrum of compound **2**

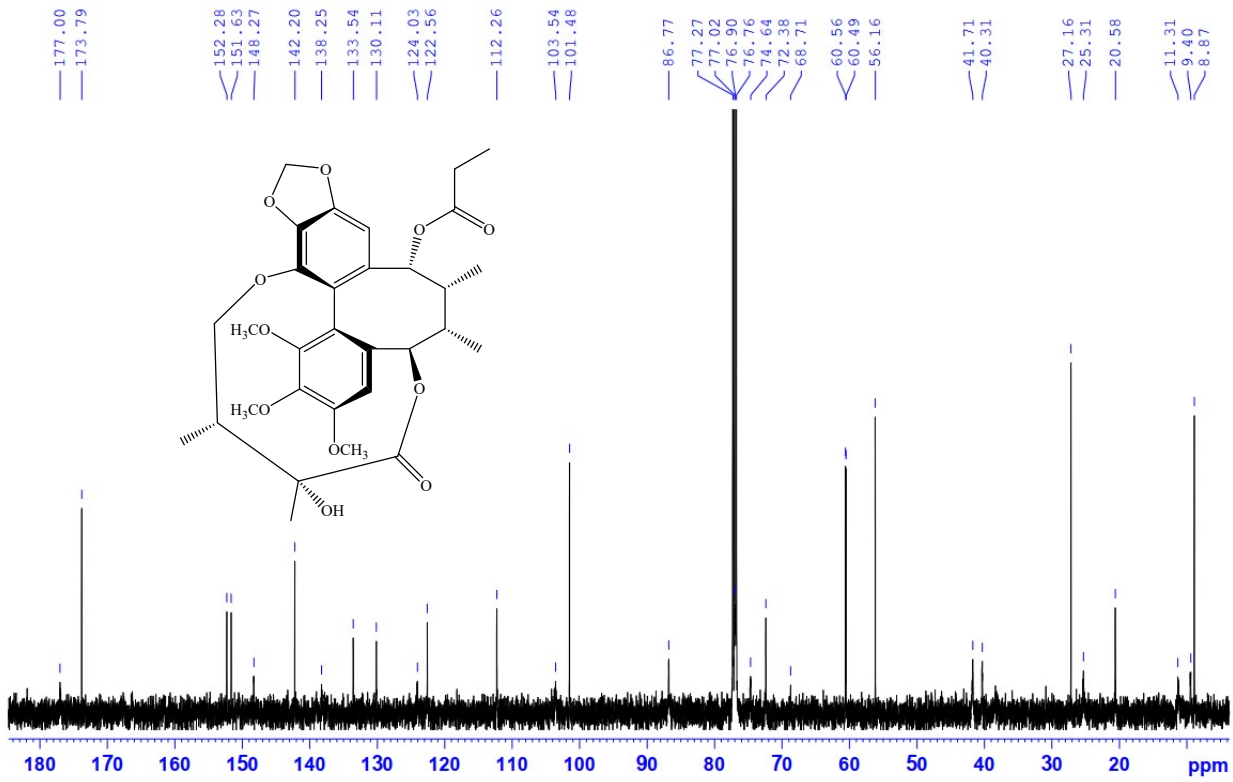

Figure S15. ^{13}C-NMR spectrum of compound **2** in CD_3OD

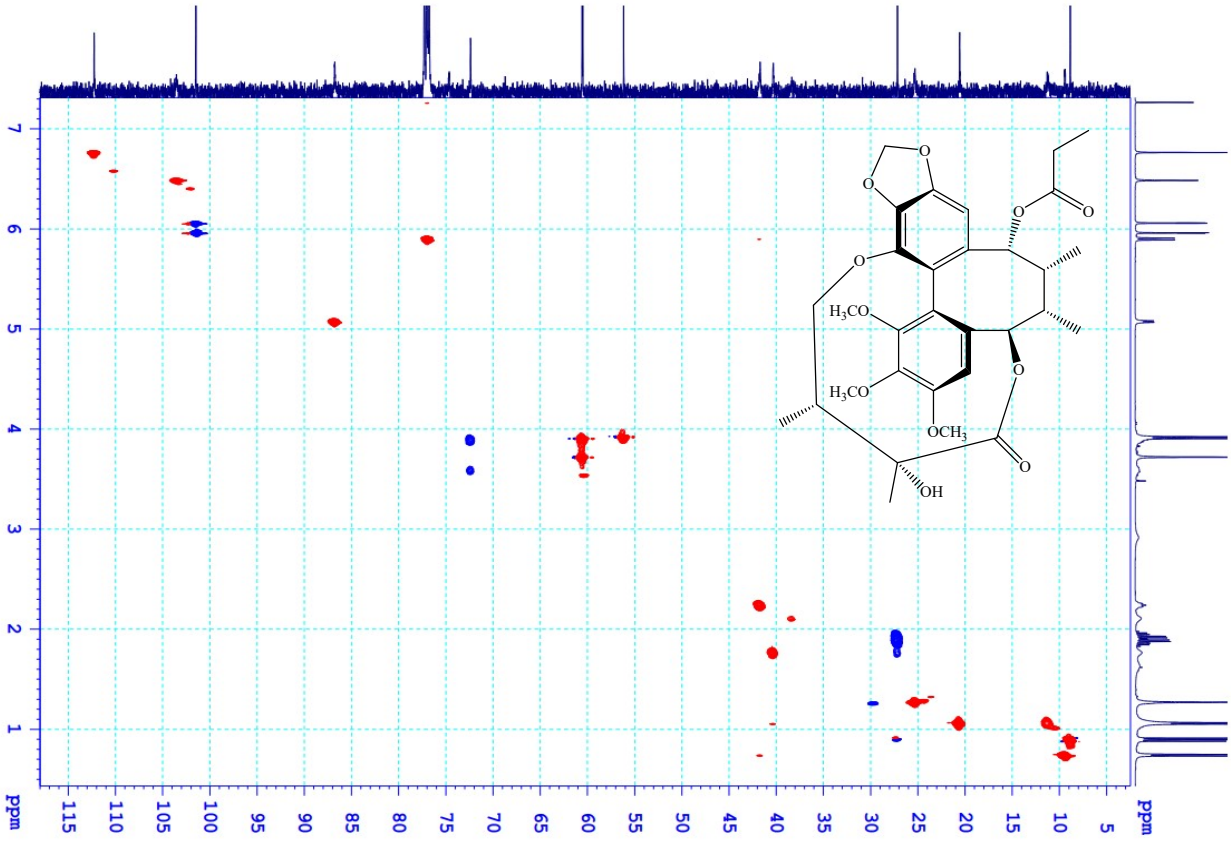

Figure S16. HSQC spectrum of compound **2**

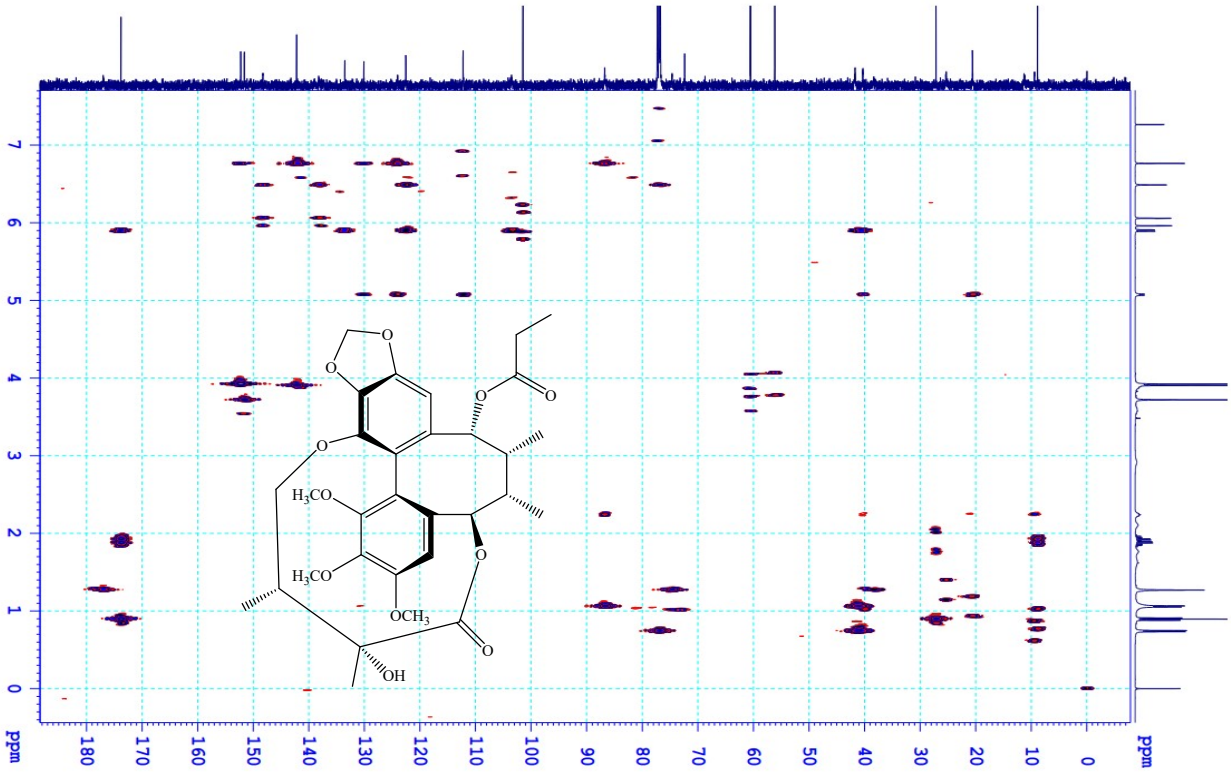

Figure S17. HMBC spectrum of compound **2**

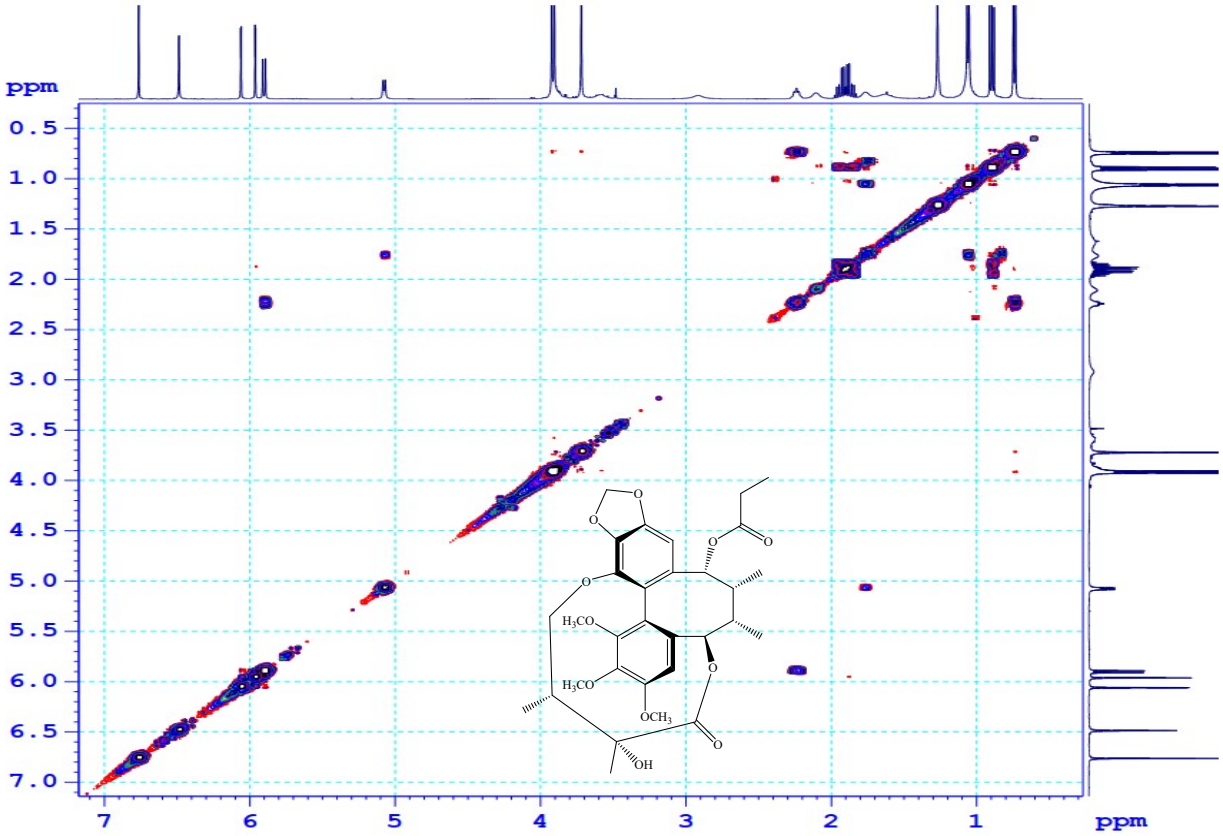

Figure S18. COSY spectrum of compound **2**

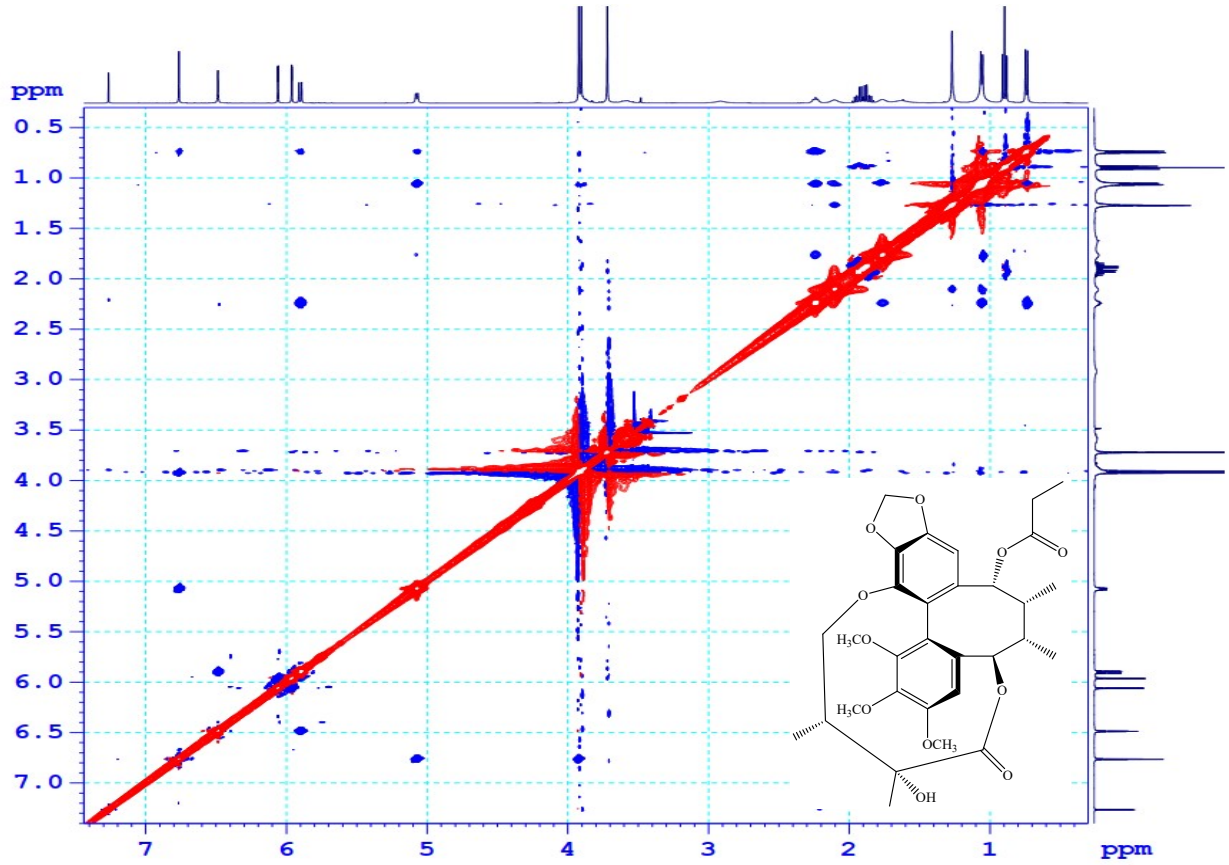

Figure S19. NOESY spectrum of compound **2**

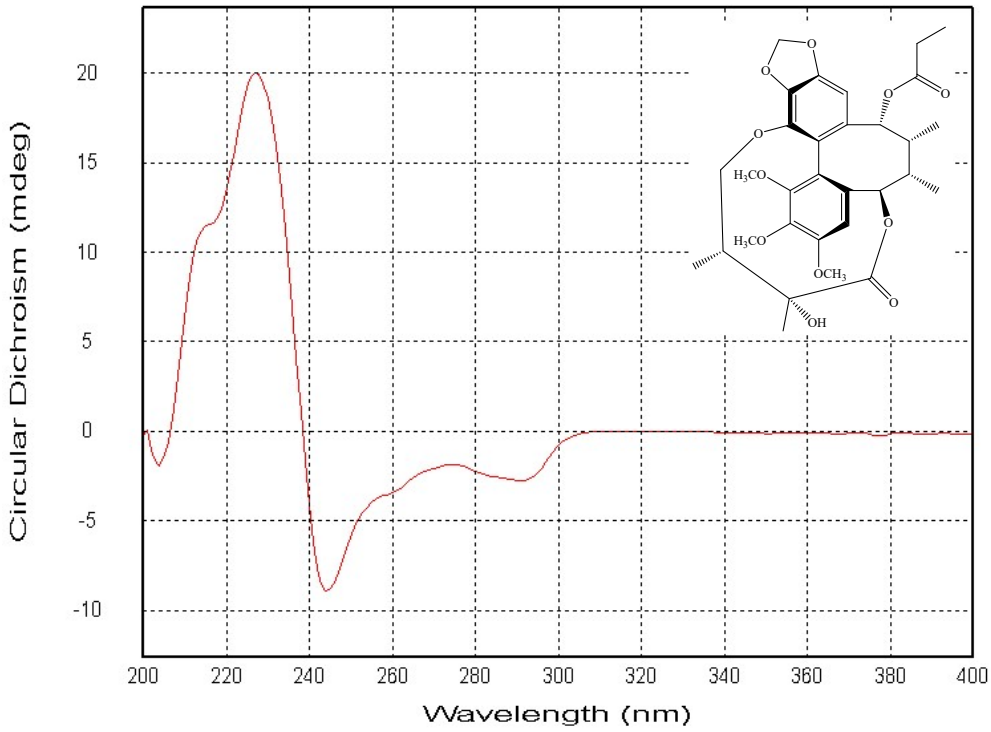

Figure S20. ECD spectrum of compound **2**

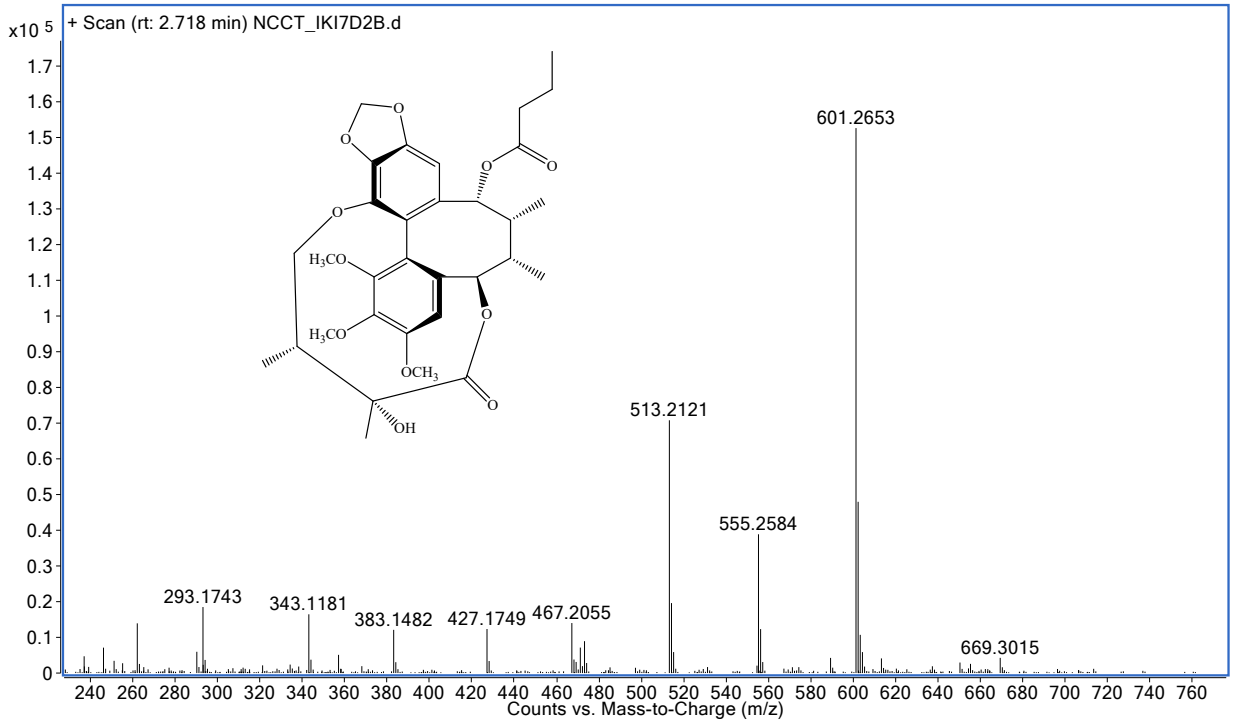

Figure S21. HR-ESI-MS of compound **3**

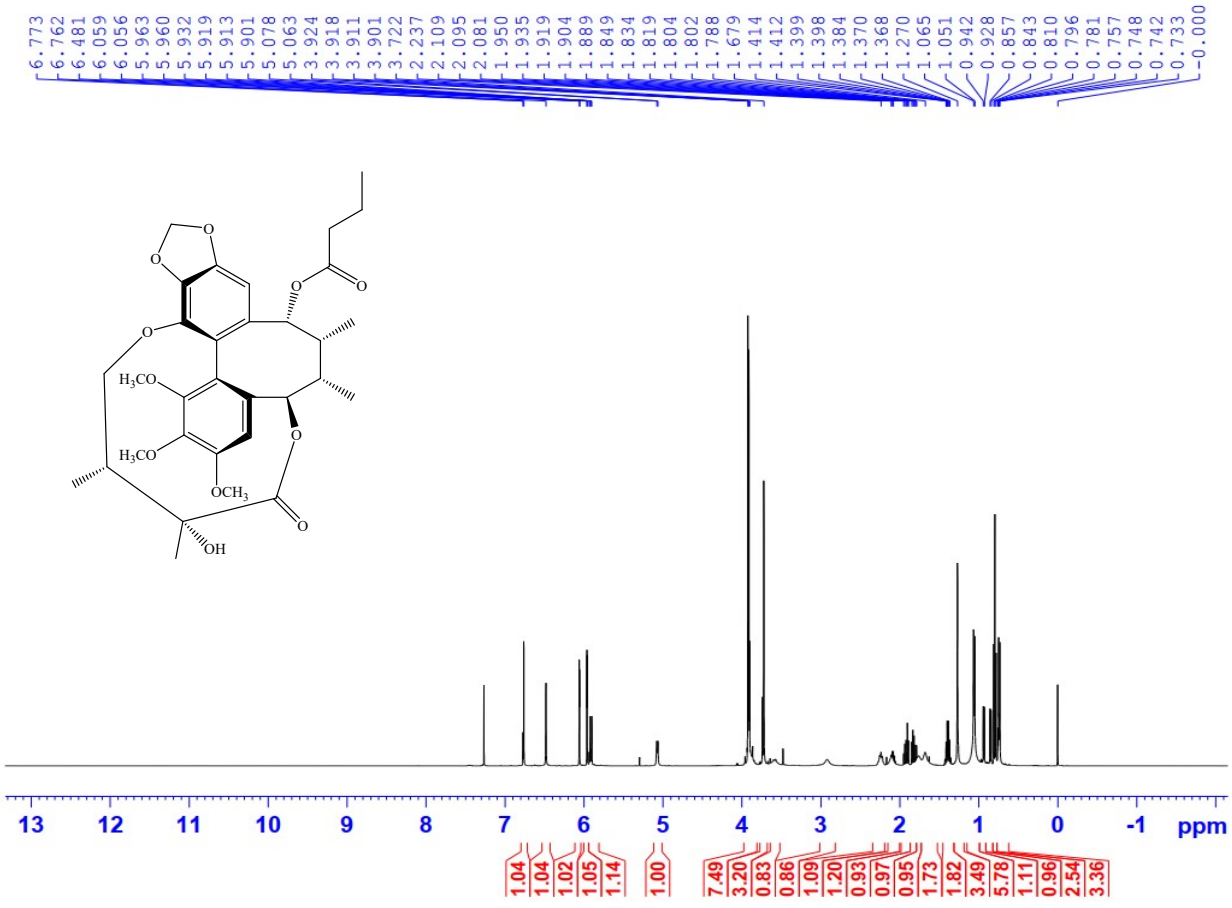

Figure S22. ^{1}H-NMR spectrum of compound **3** in $CDCl_3$

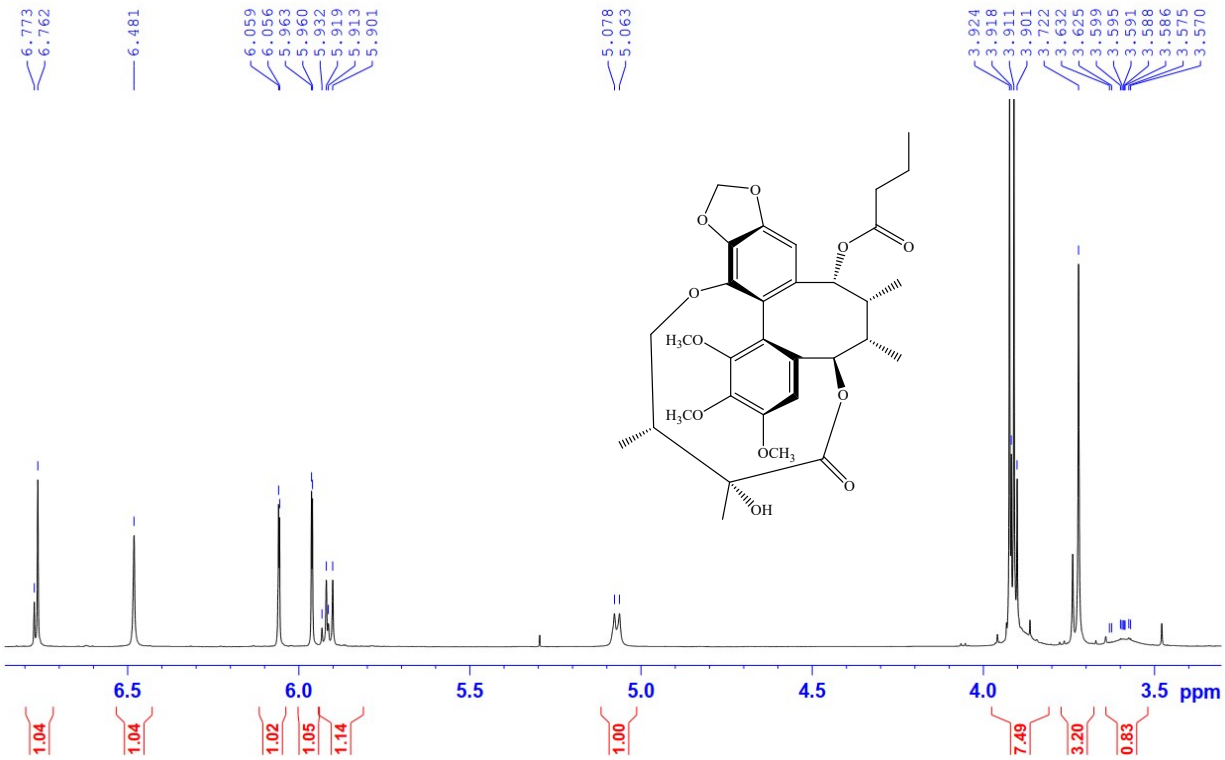

Figure S23. Expanded [1]H-NMR spectrum of compound **3**

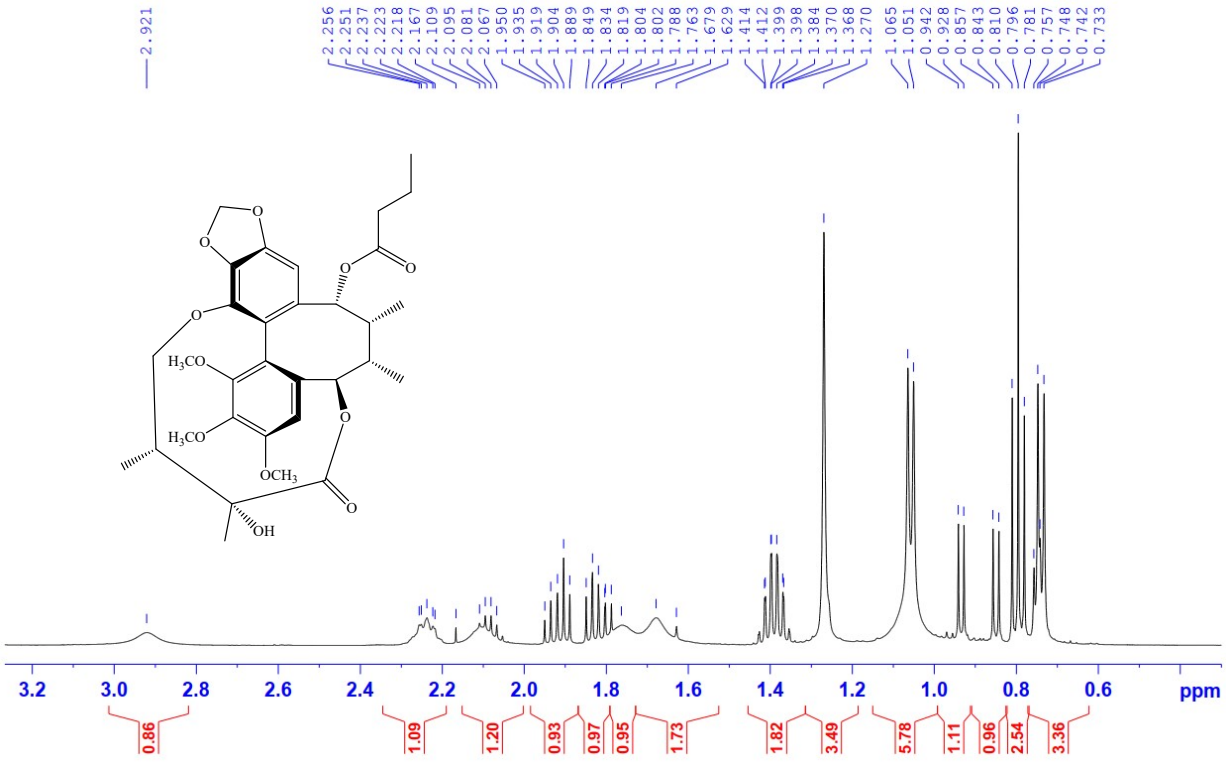

Figure S24. Expanded [1]H-NMR spectrum of compound **3**

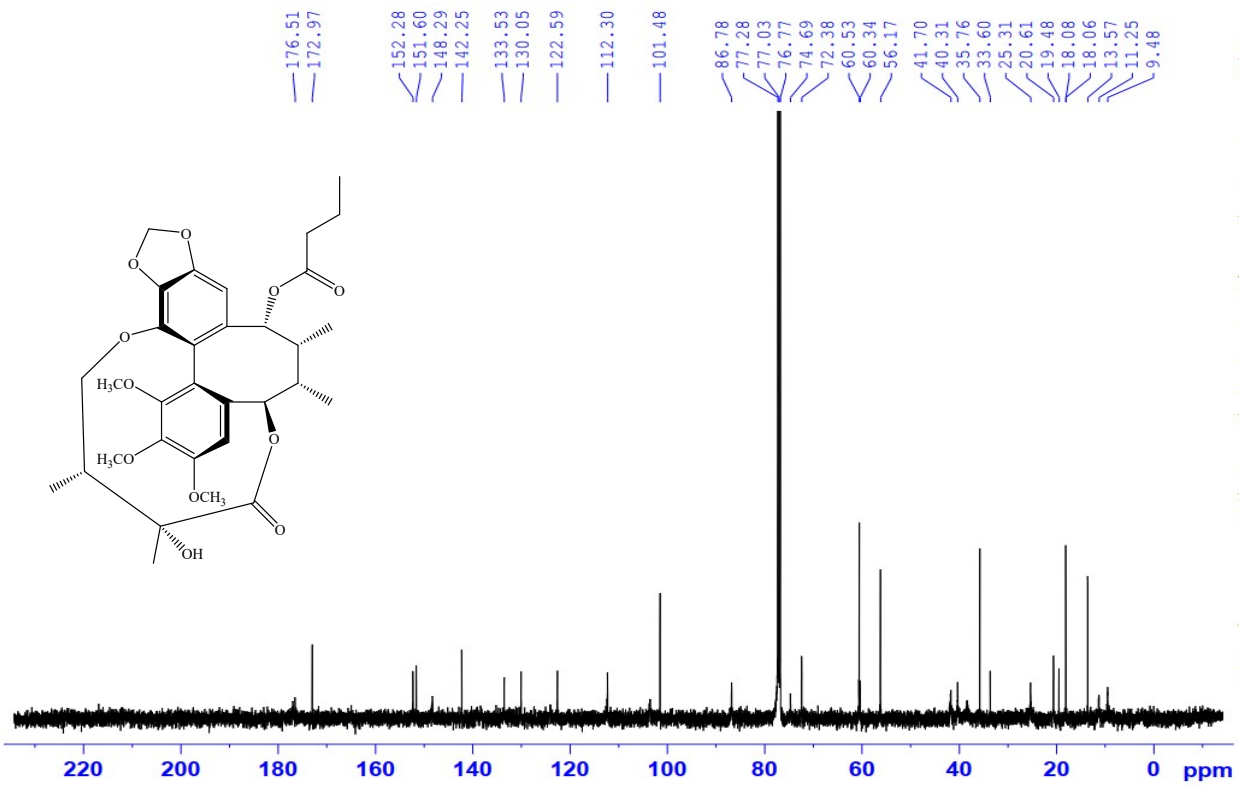

Figure S25. ^{13}C-NMR spectrum of compound **3** in CD_3OD

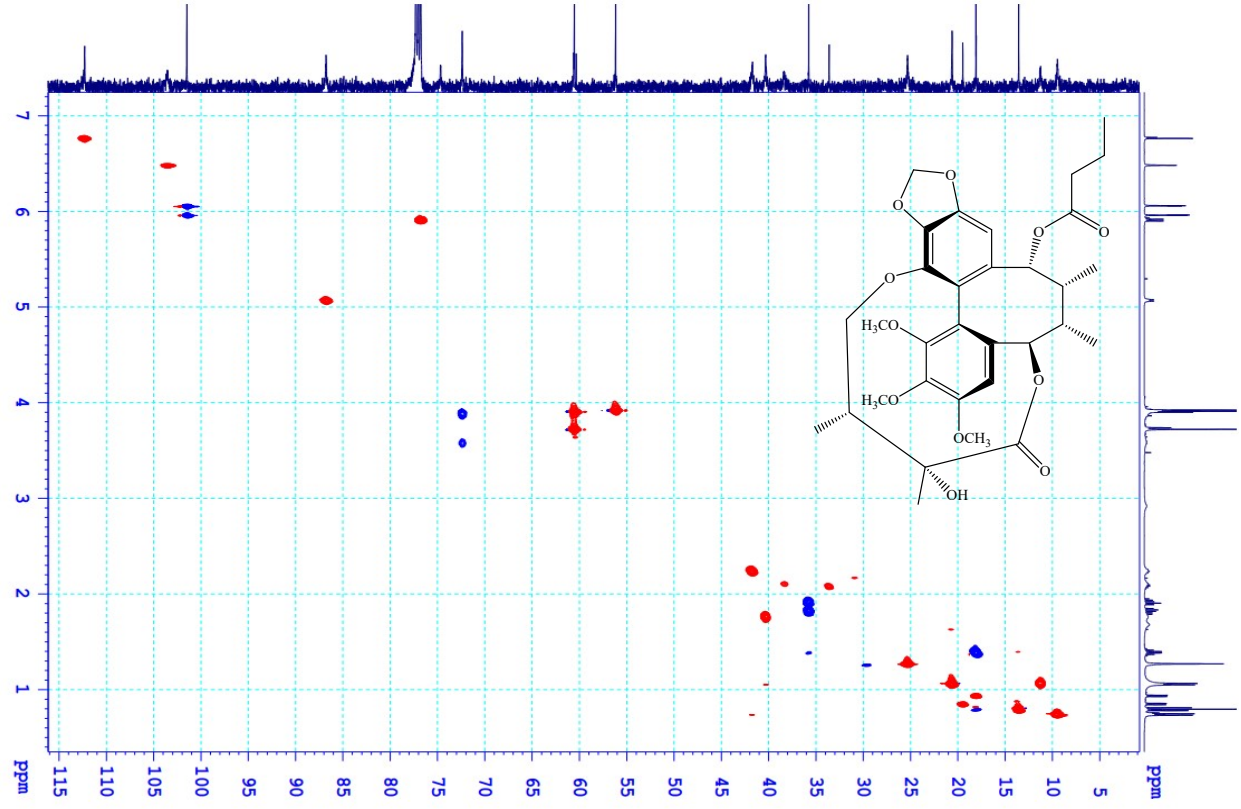

Figure S26. HSQC spectrum of compound **3**

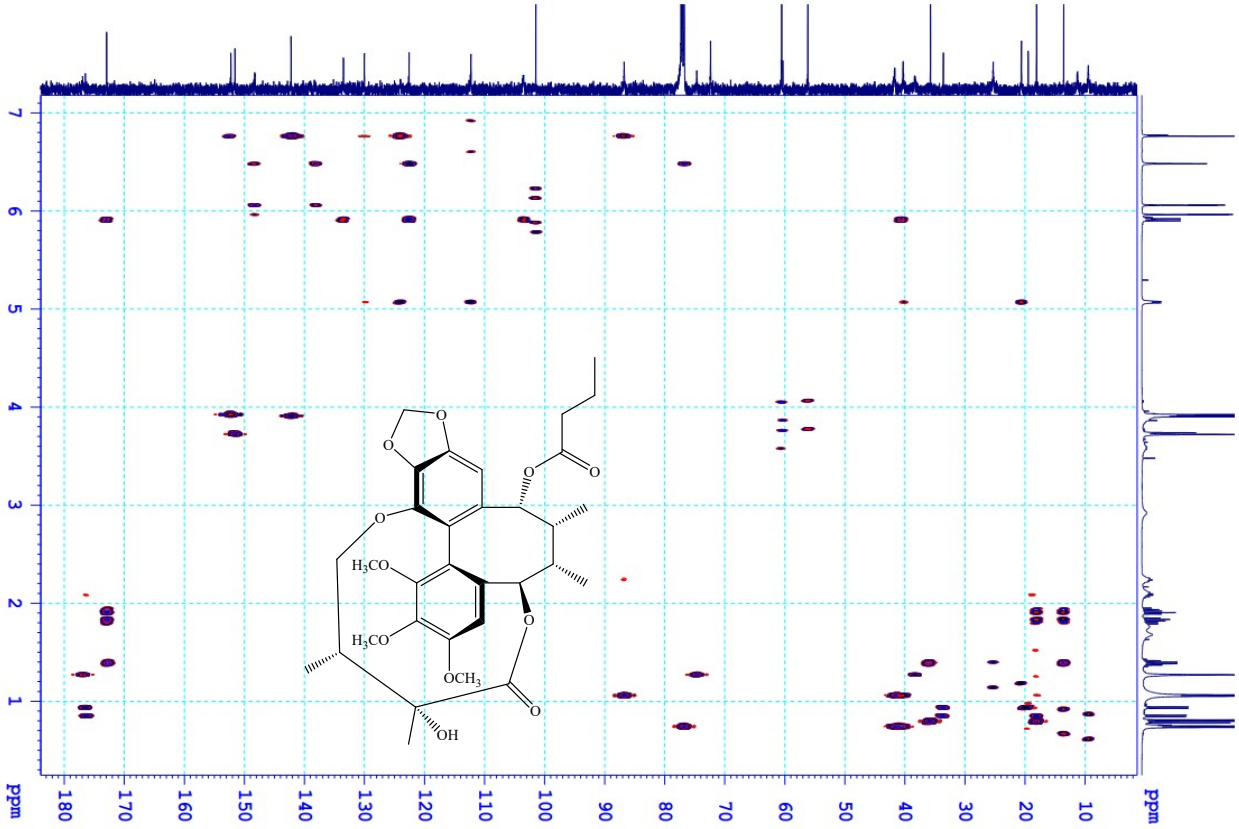

Figure S27. HMBC spectrum of compound **3**

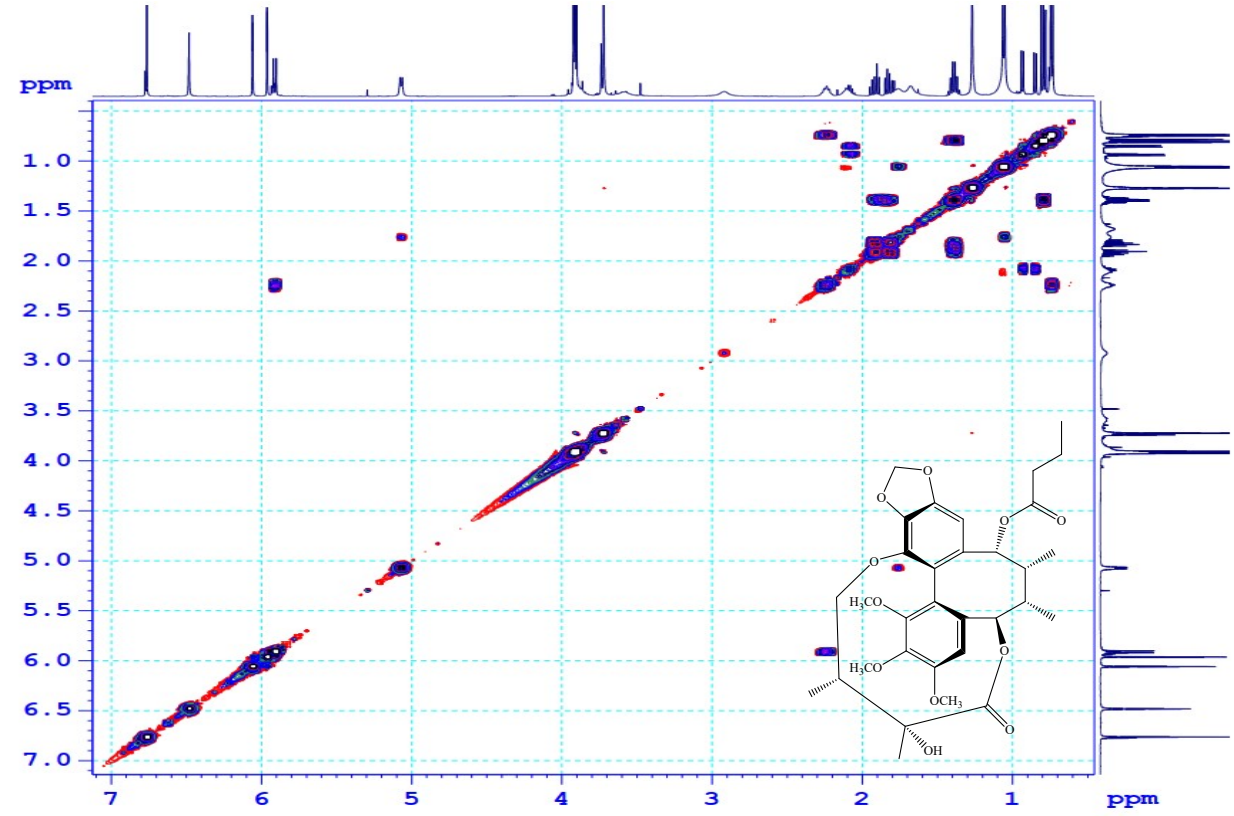

Figure S28. COSY spectrum of compound **3**

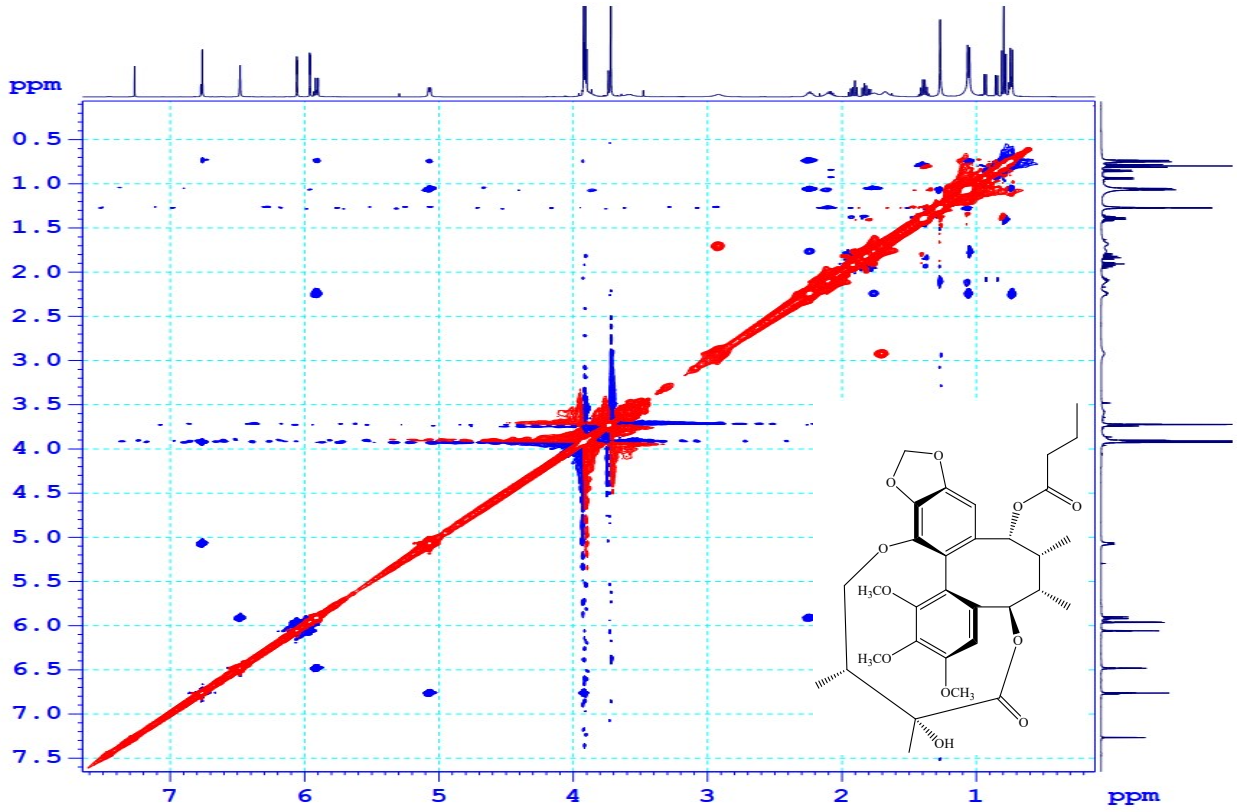

Figure S29. NOESY spectrum of compound **3**

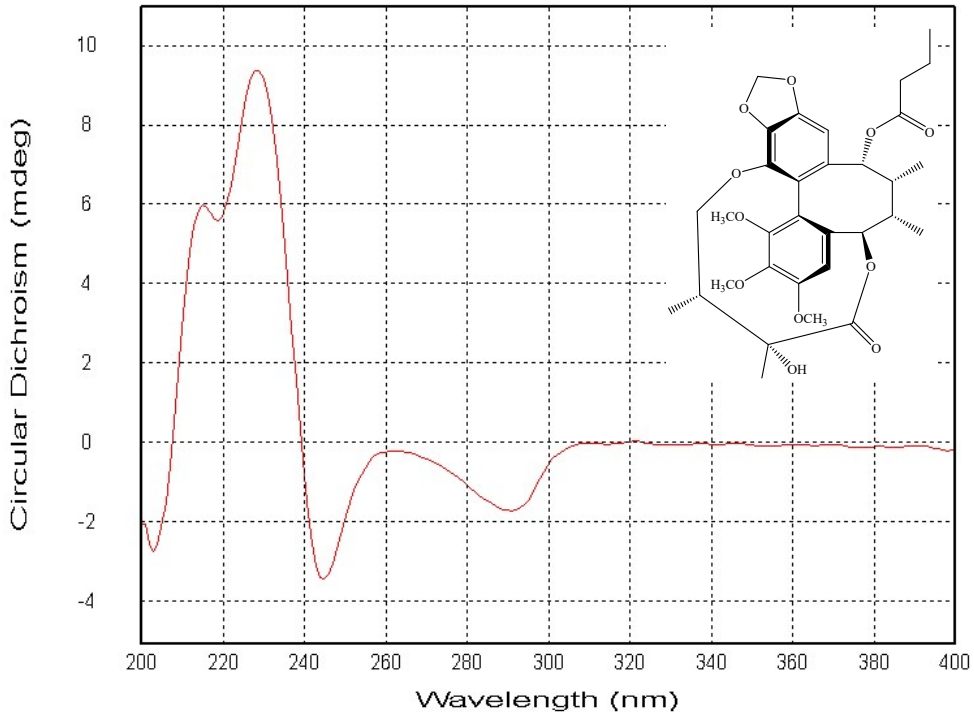

Figure S30. ECD spectrum of compound **3**

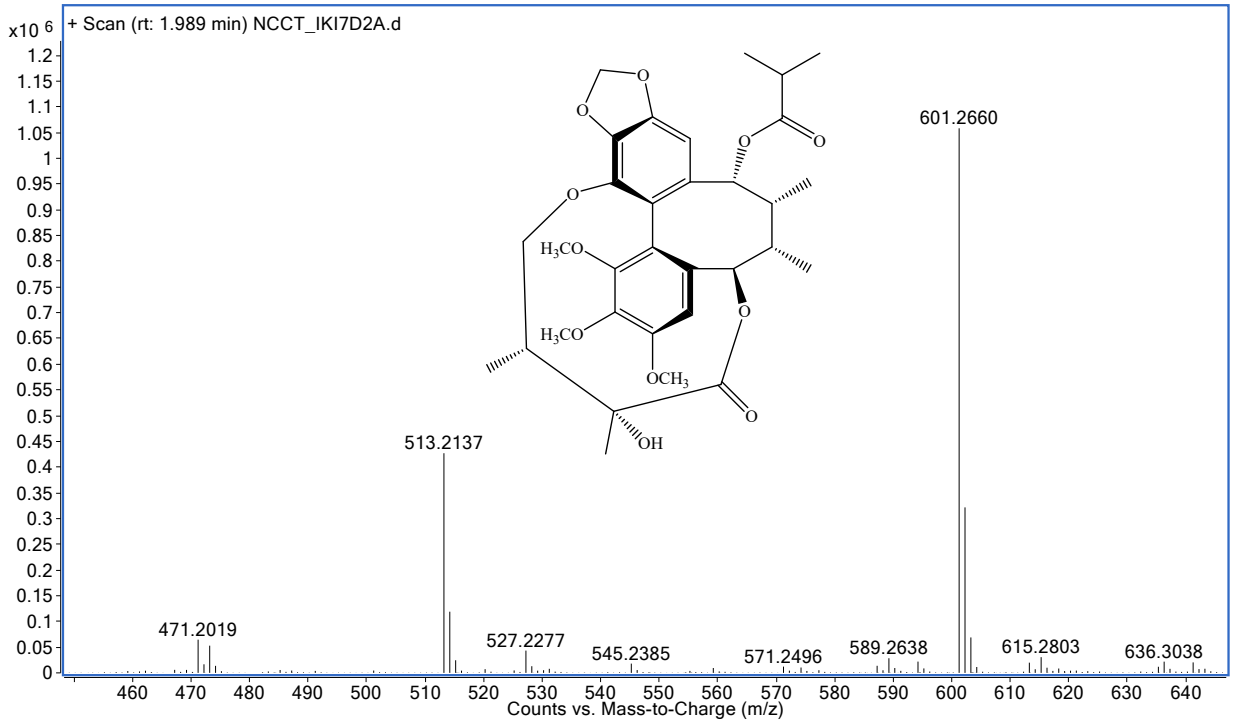

Figure S31. HR-ESI-MS of compound **4**

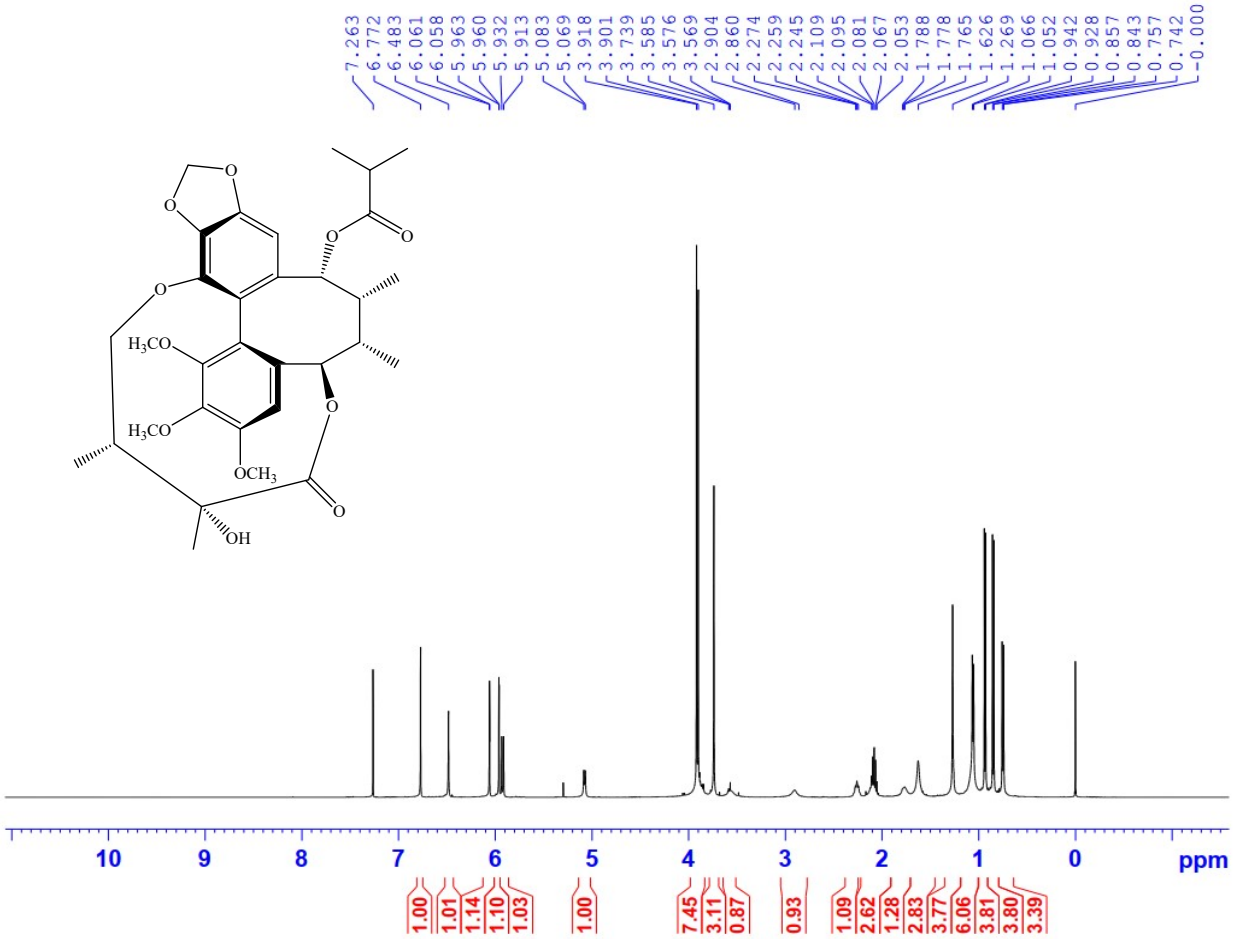

Figure S32. ^{1}H-NMR spectrum of compound **4** in $CDCl_3$

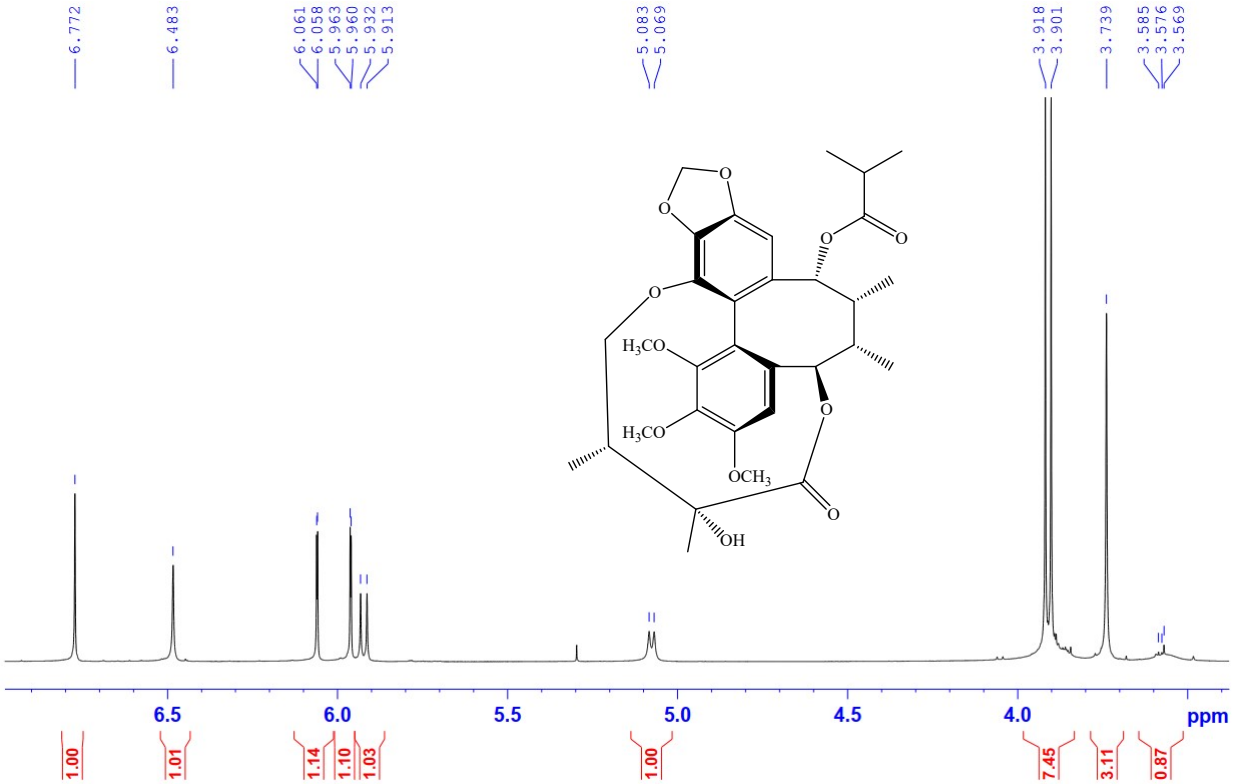

Figure S33. Expanded ^{1}H-NMR spectrum of compound **4**

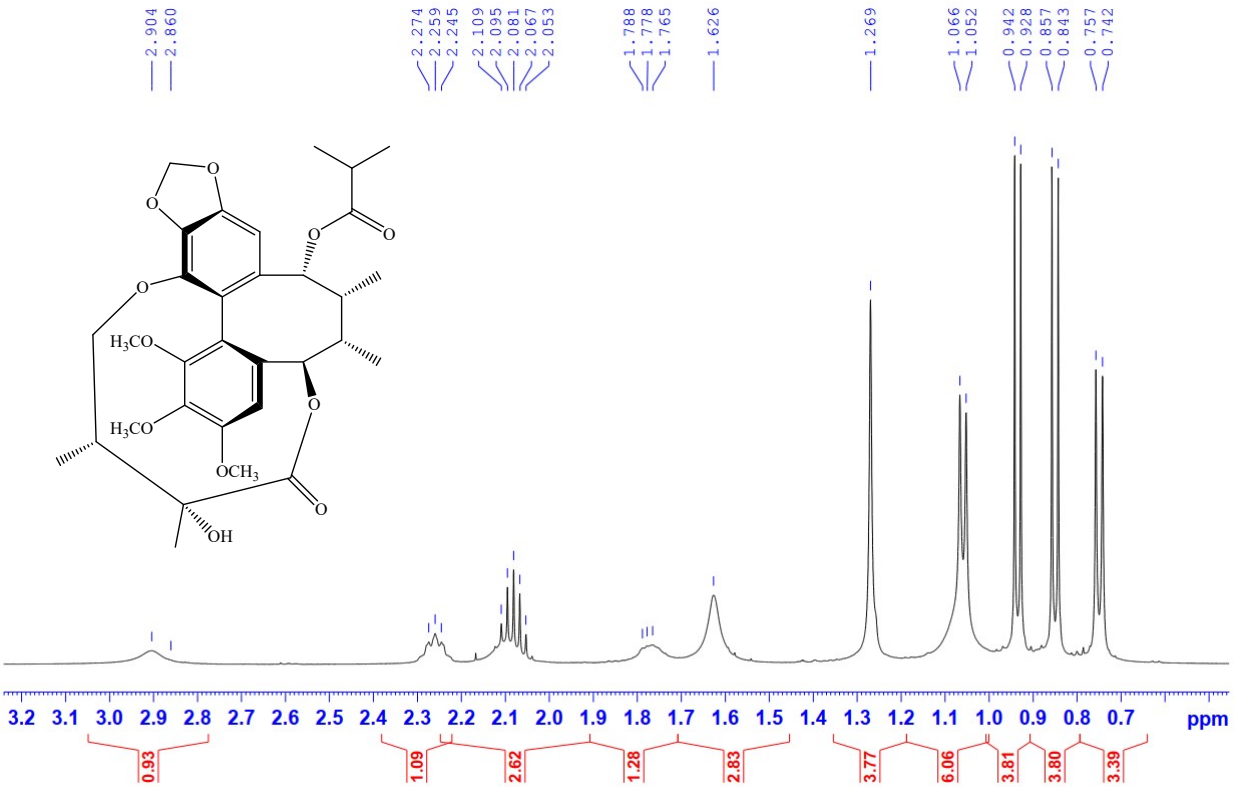

Figure S34. Expanded [1]H-NMR spectrum of compound **4**

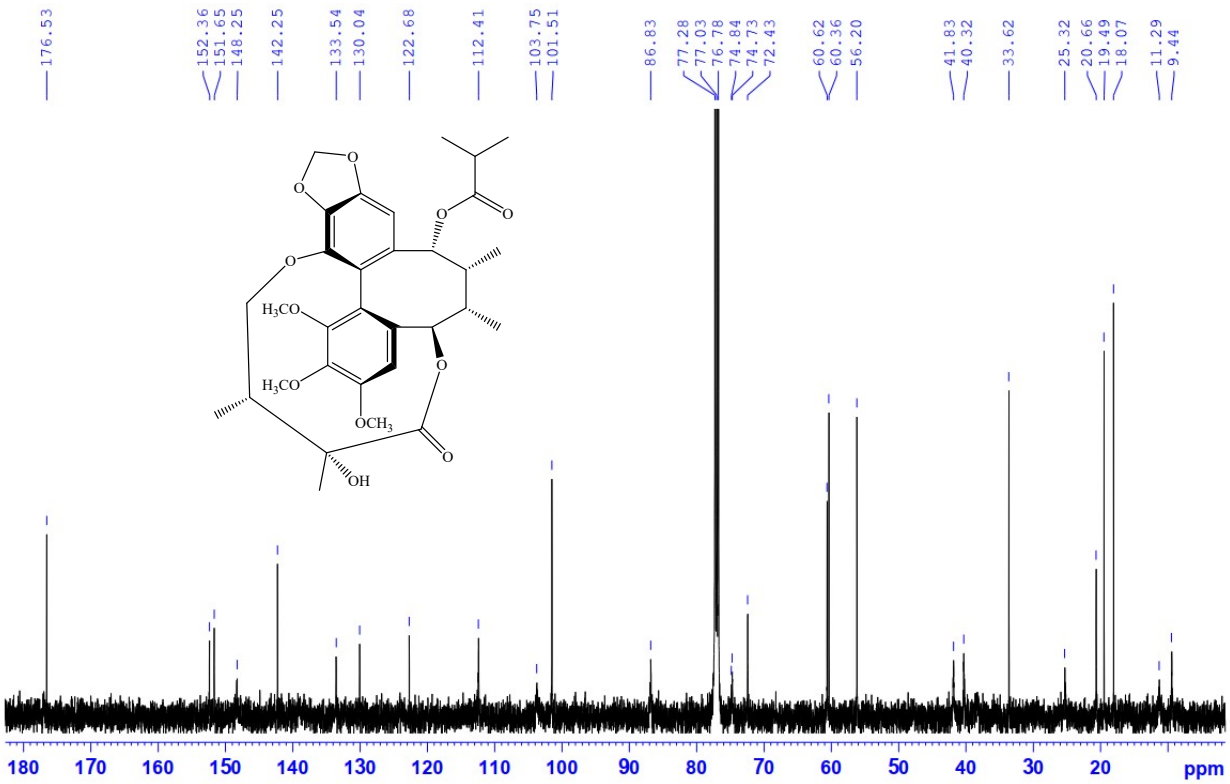

Figure S35. ^{13}C-NMR spectrum of compound **4** in $CDCl_3$

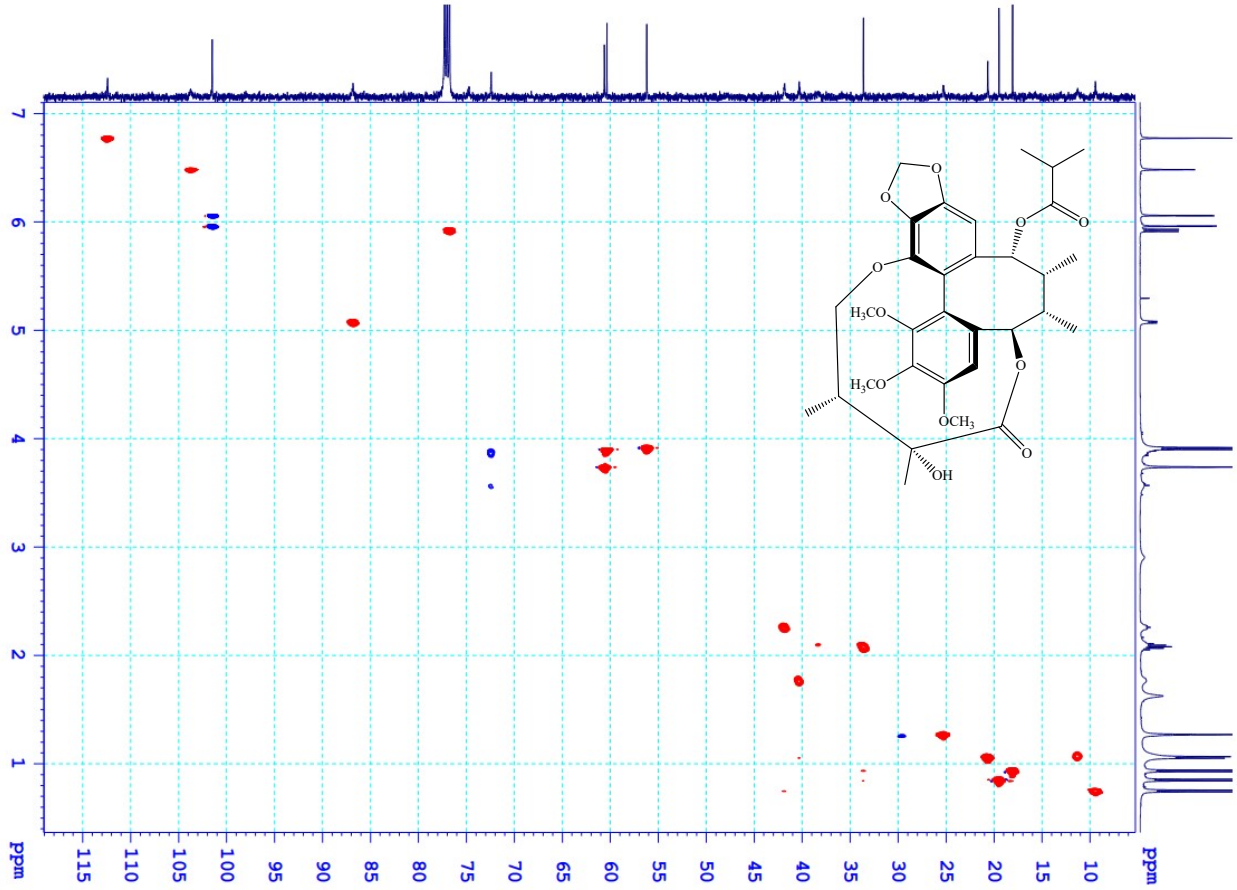

Figure S36. HSQC spectrum of compound **4**

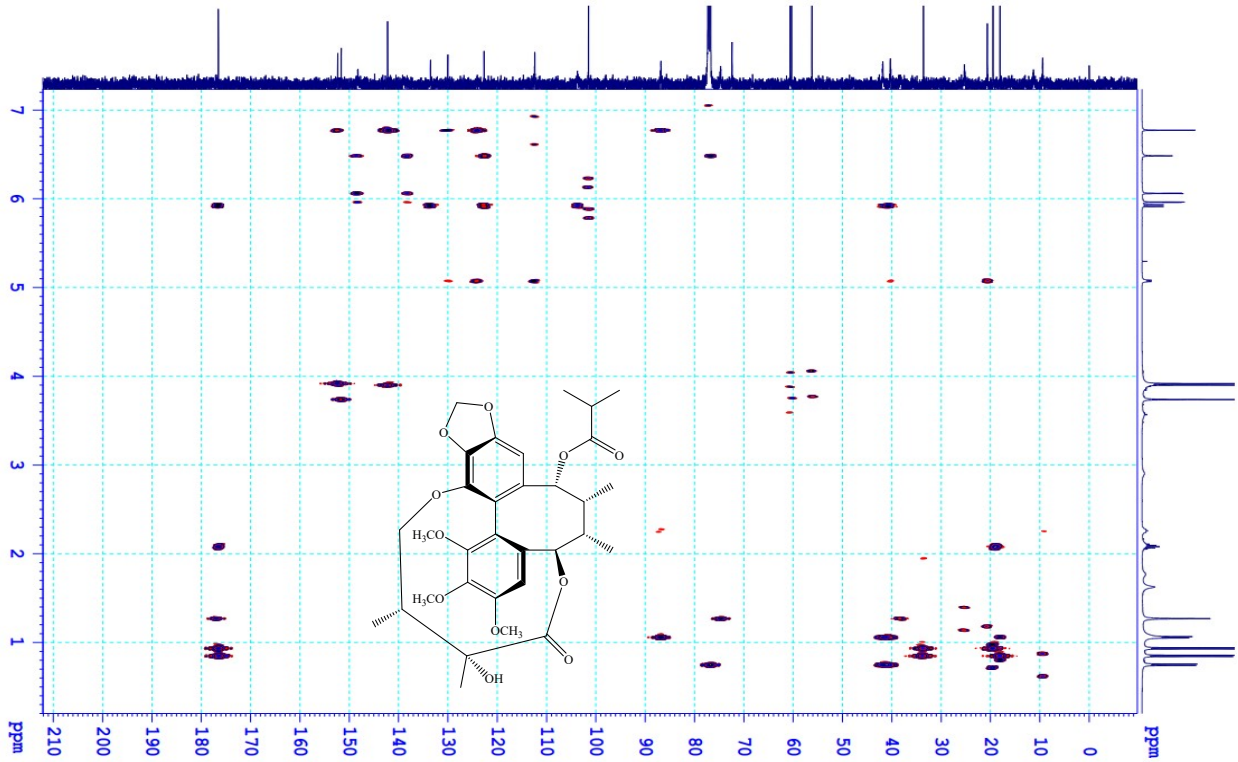

Figure S37. HMBC spectrum of compound **4**

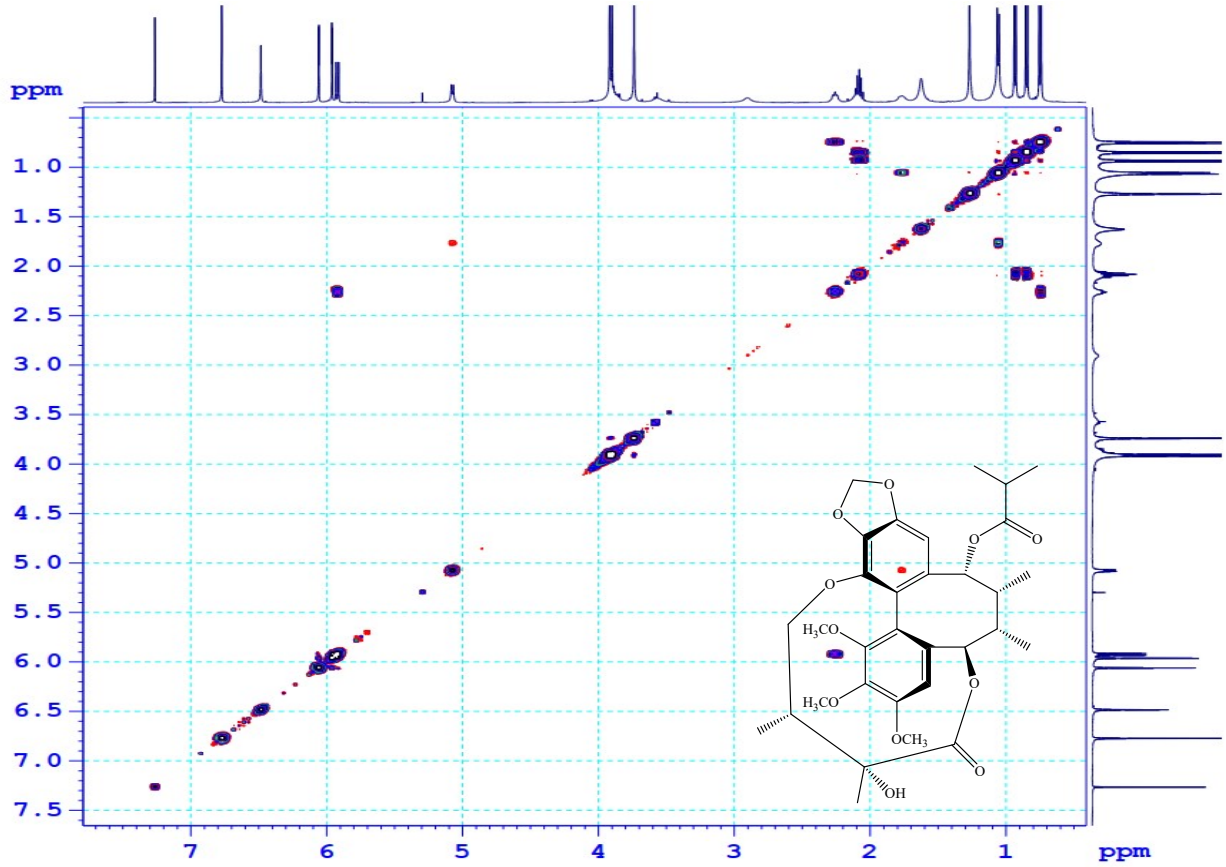

Figure S38. COSY spectrum of compound **4**

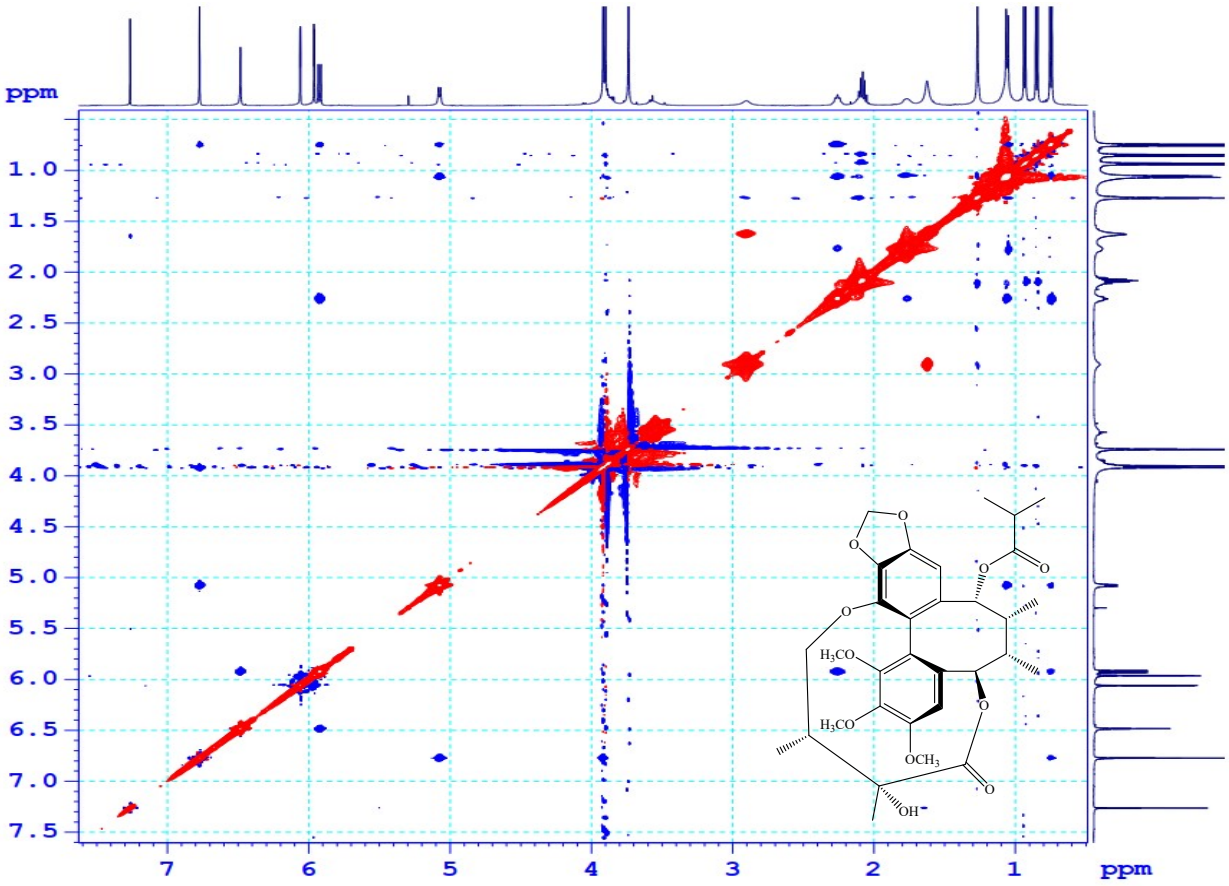

Figure S39. NOESY spectrum of compound **4**

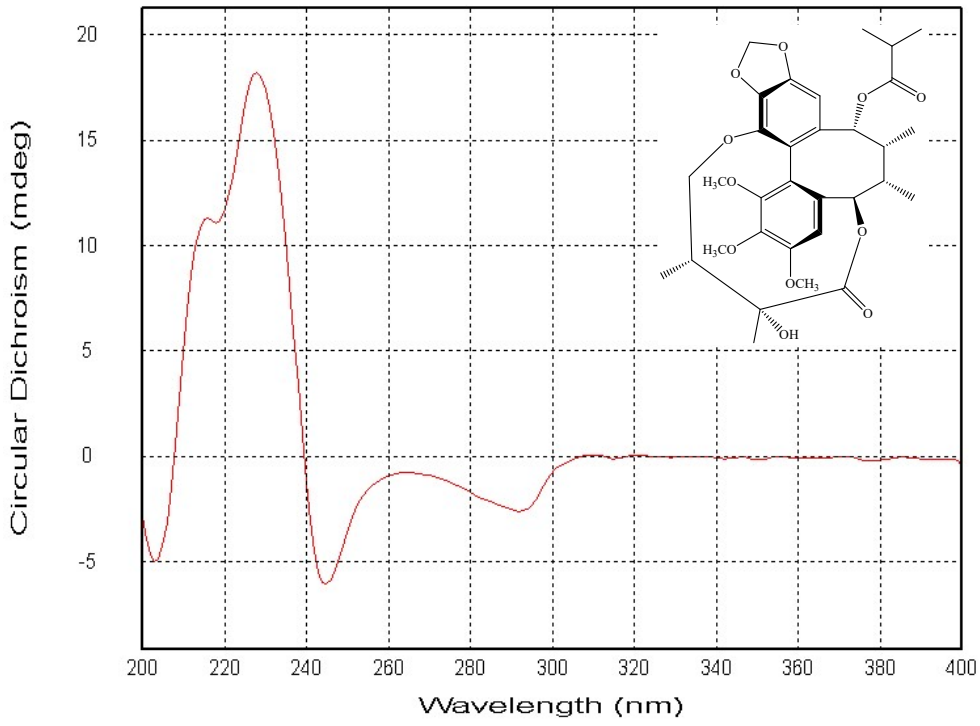

Figure S40. ECD spectrum of compound **4**

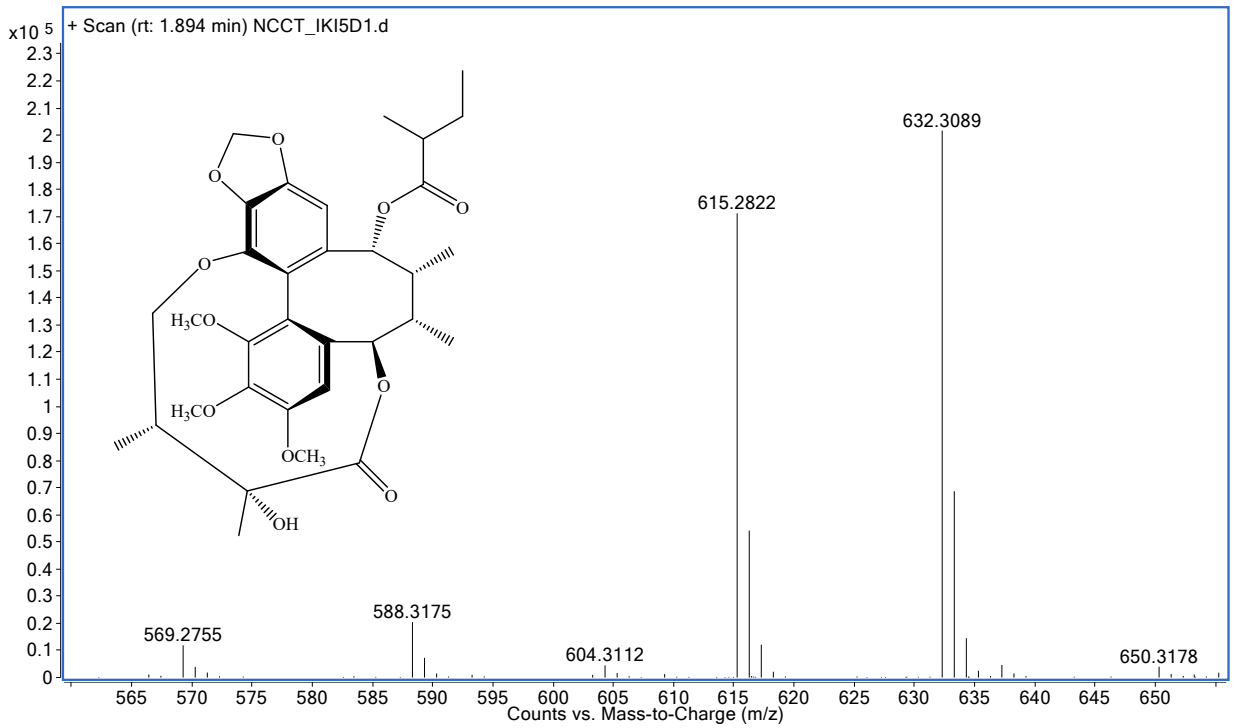

Figure S41. HR-ESI-MS of compound **5**

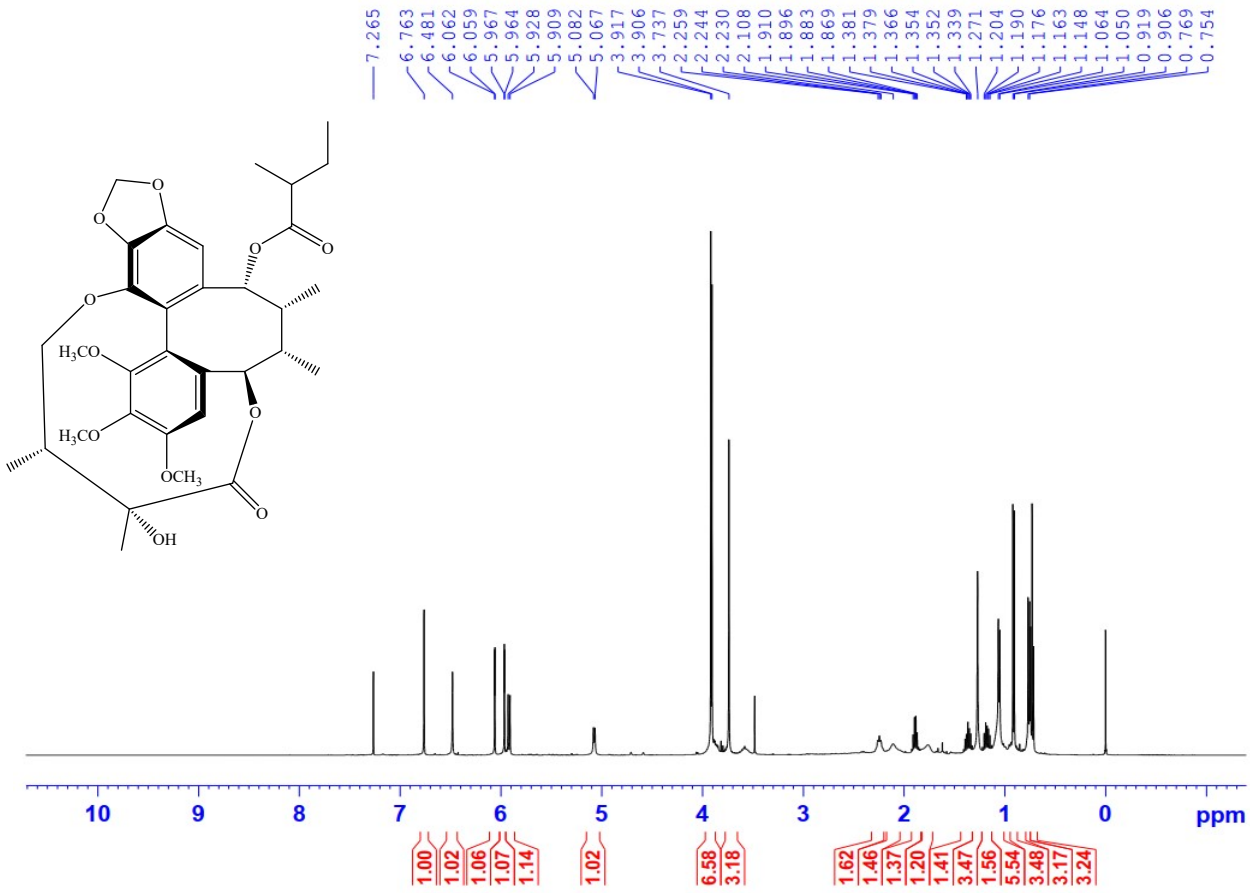

Figure S42. ^{1}H-NMR spectrum of compound **5** in $CDCl_3$

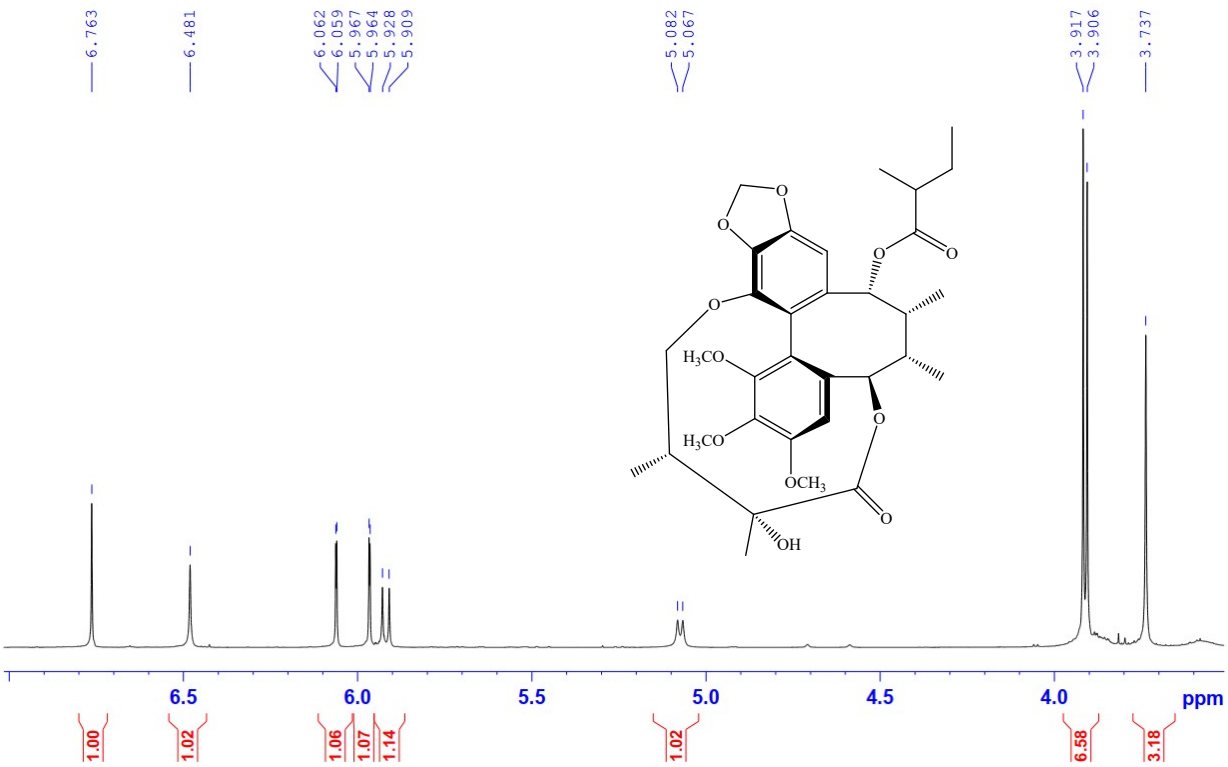

Figure S43. Expanded [1]H-NMR spectrum of compound **5**

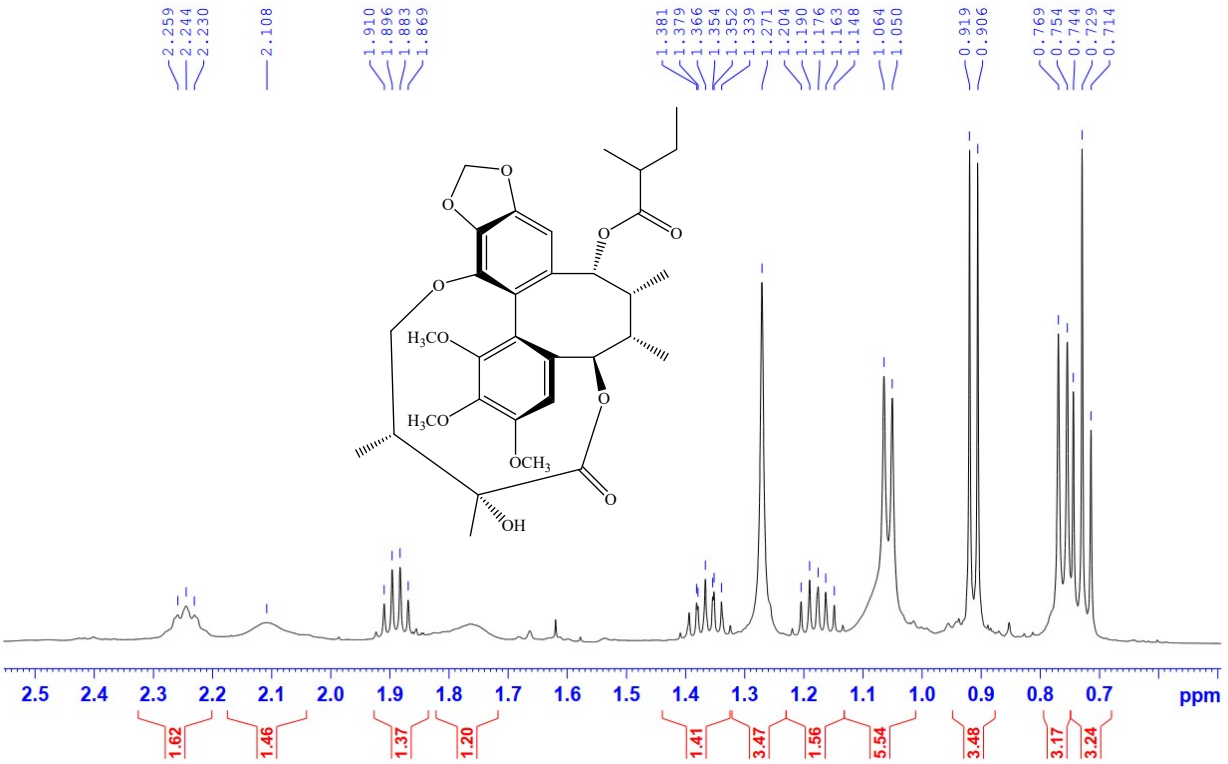

Figure S44. Expanded [1]H-NMR spectrum of compound **5**

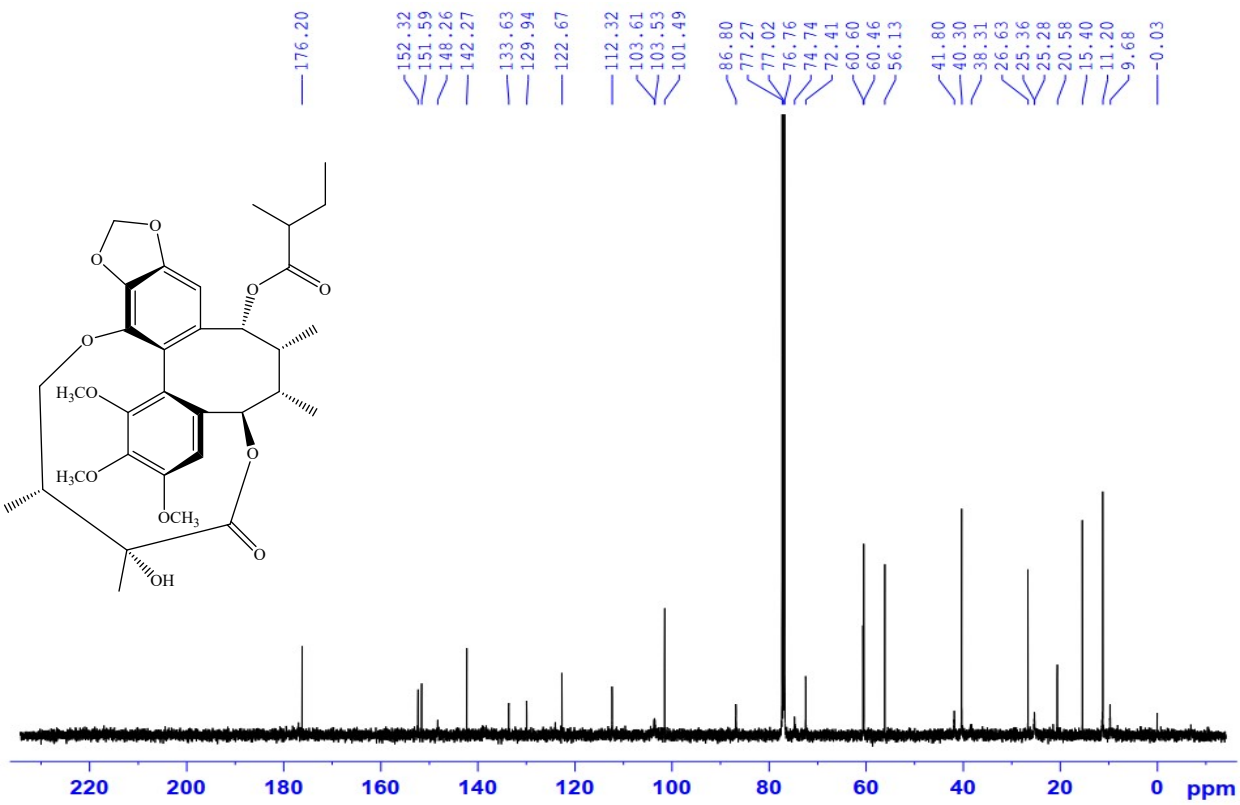

Figure S45. ^{13}C-NMR spectrum of compound **5** in $CDCl_3$

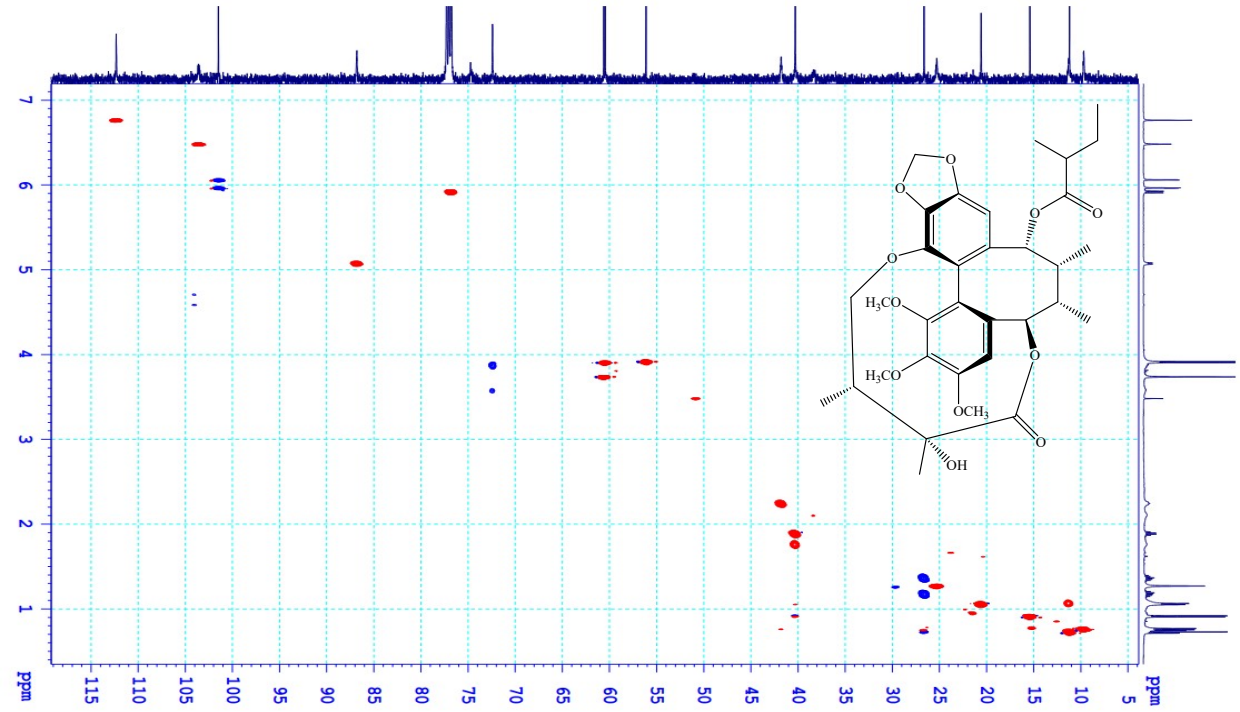

Figure S46. HSQC spectrum of compound **5**

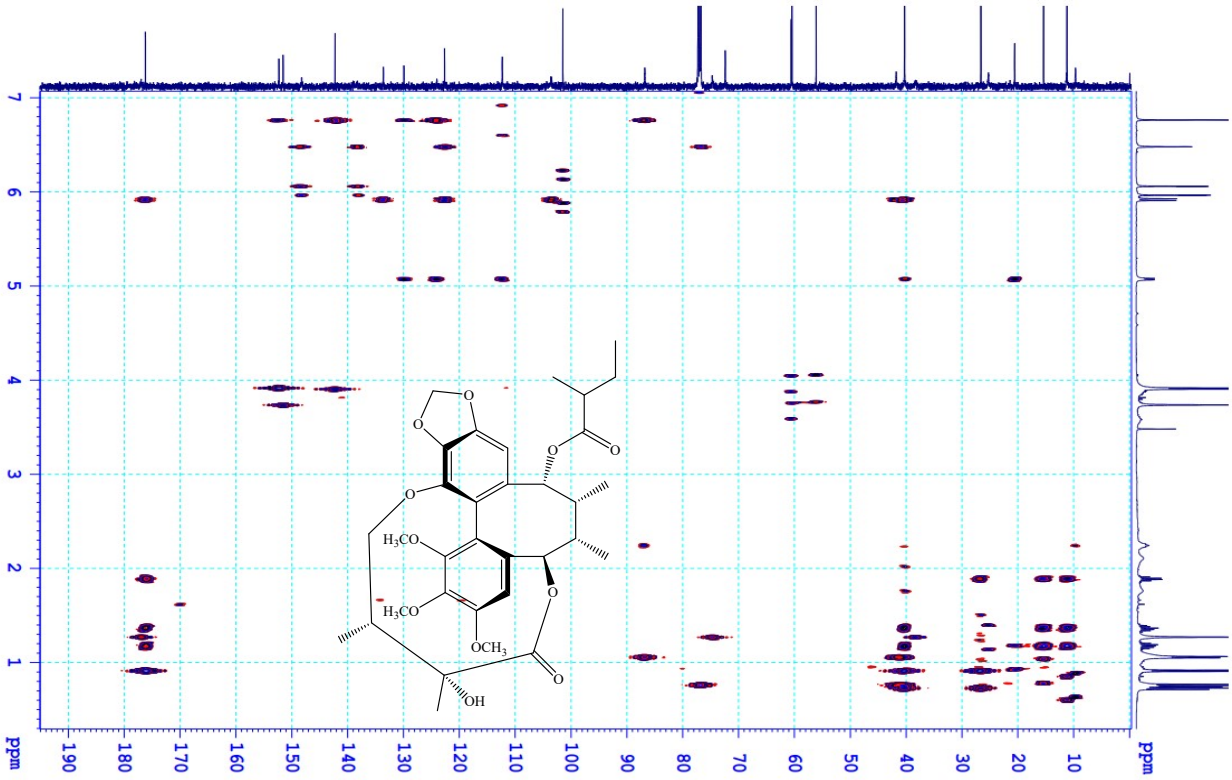

Figure S47. HMBC spectrum of compound **5**

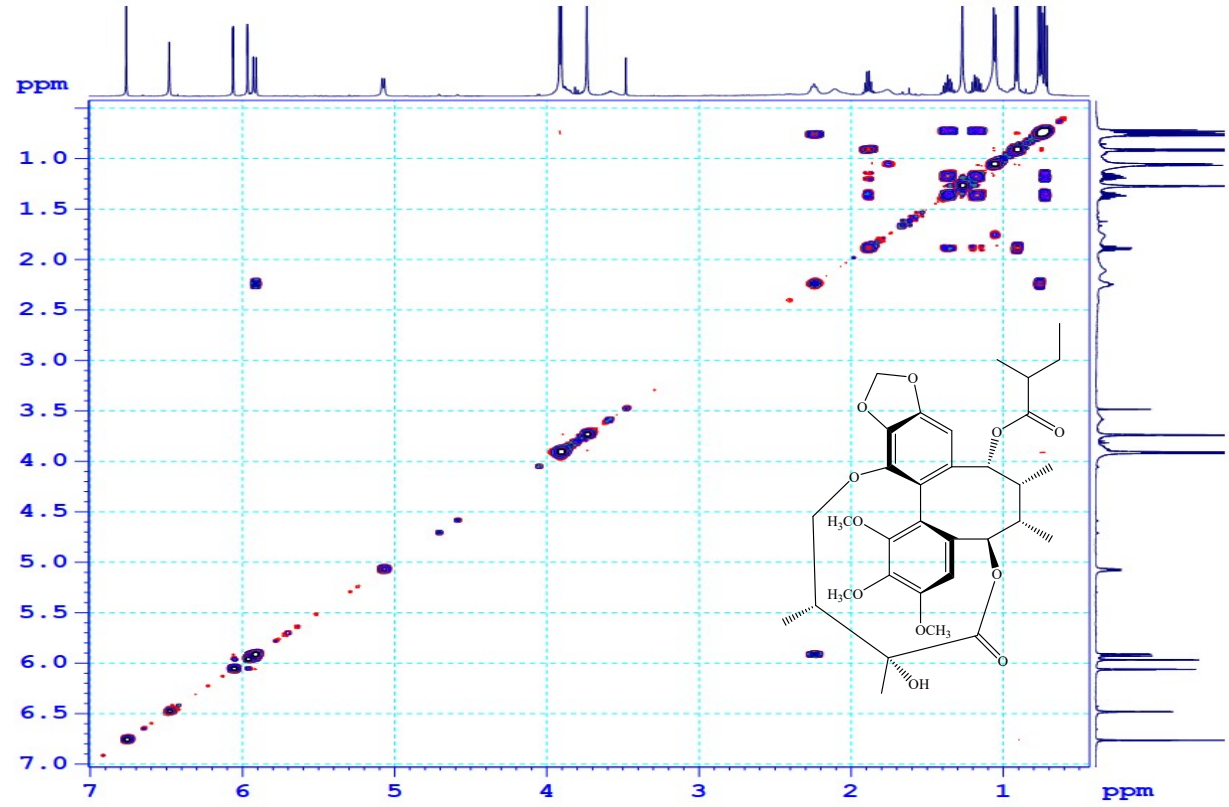

Figure S48. COSY spectrum of compound **5**

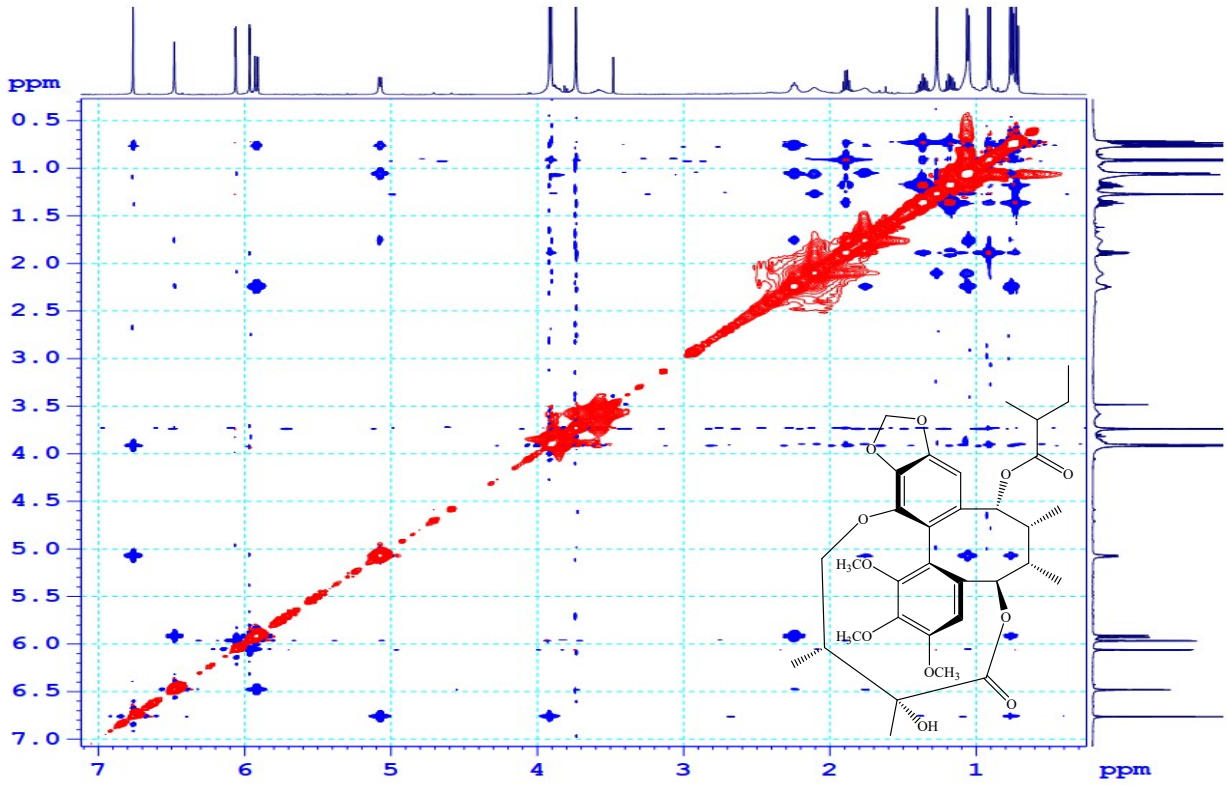

Figure S49. NOESY spectrum of compound **5**

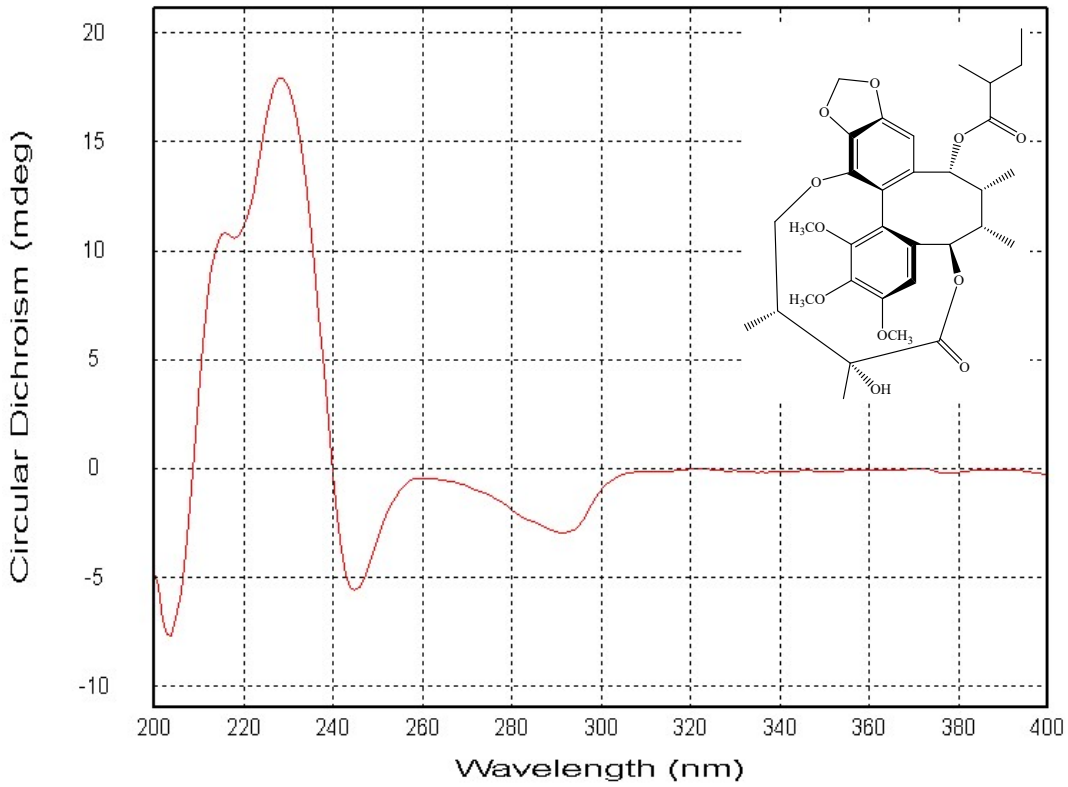

Figure S50. ECD spectrum of compound **5**

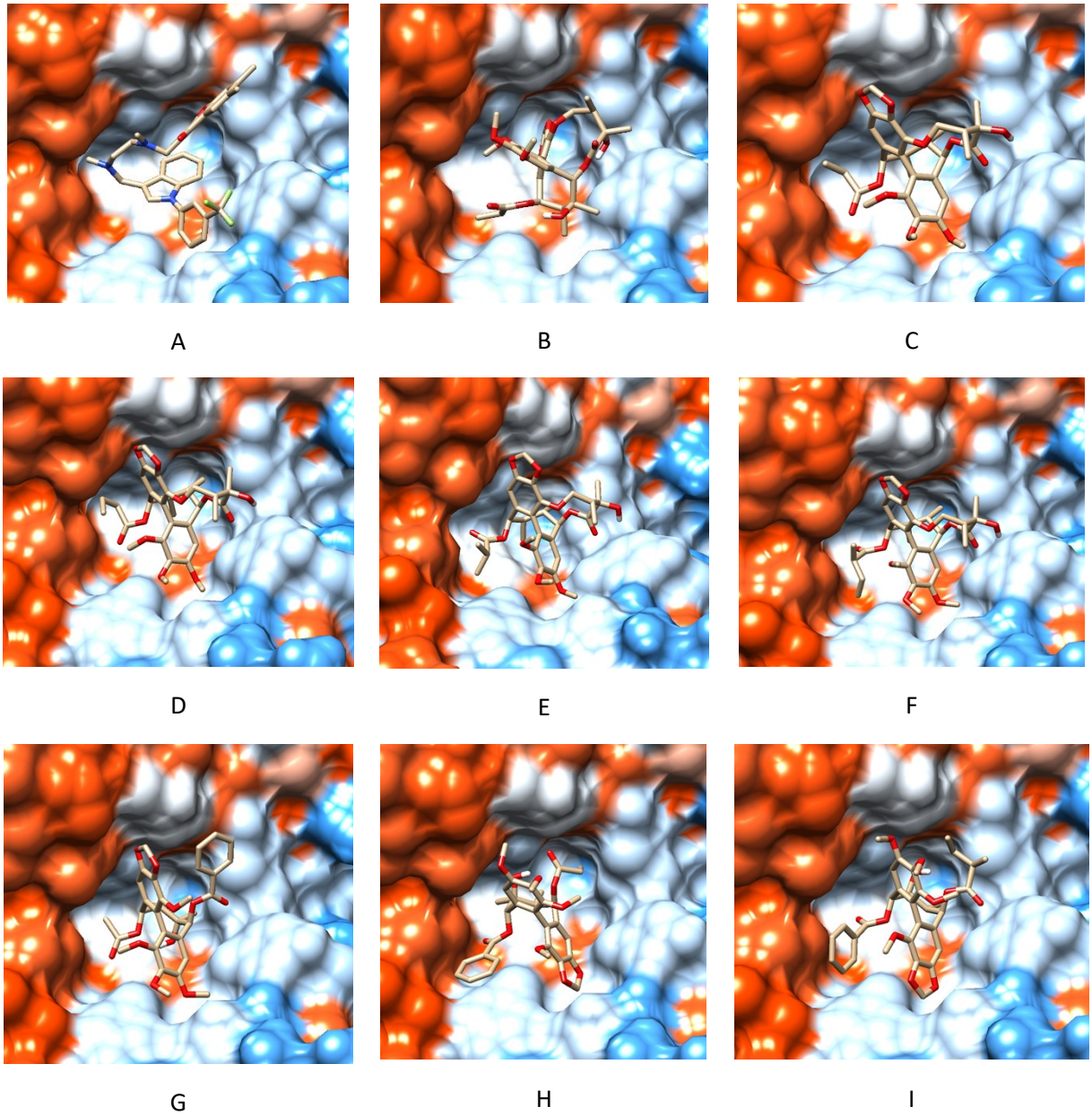

Figure S51. Docking pose of positive drug 307 (A) and compounds **1**-**8** (B-I) on TNF-α

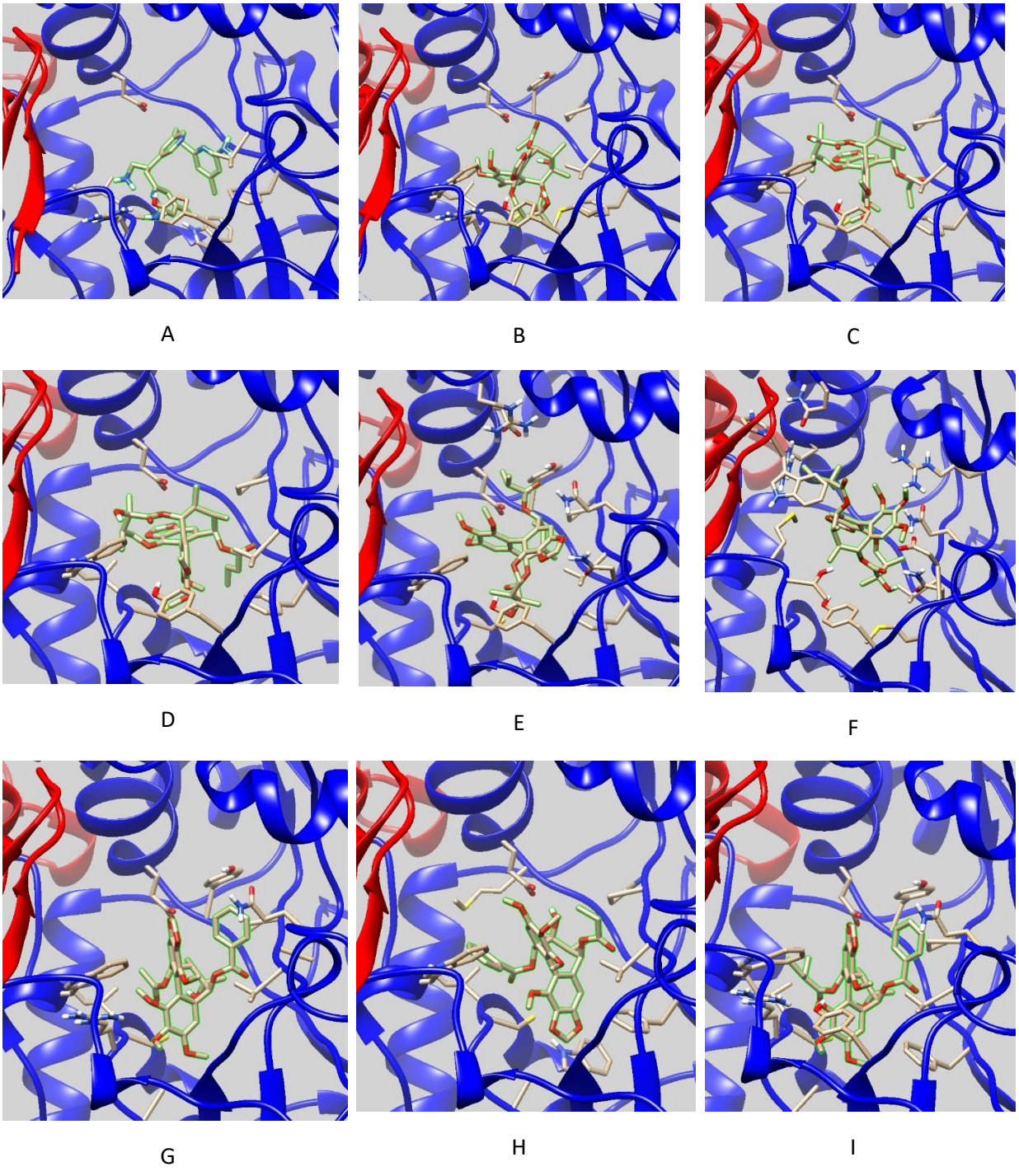

Figure S52. Docking pose of positive drug S71 (A) and compounds **1**-**8** (B-I) on iNOS

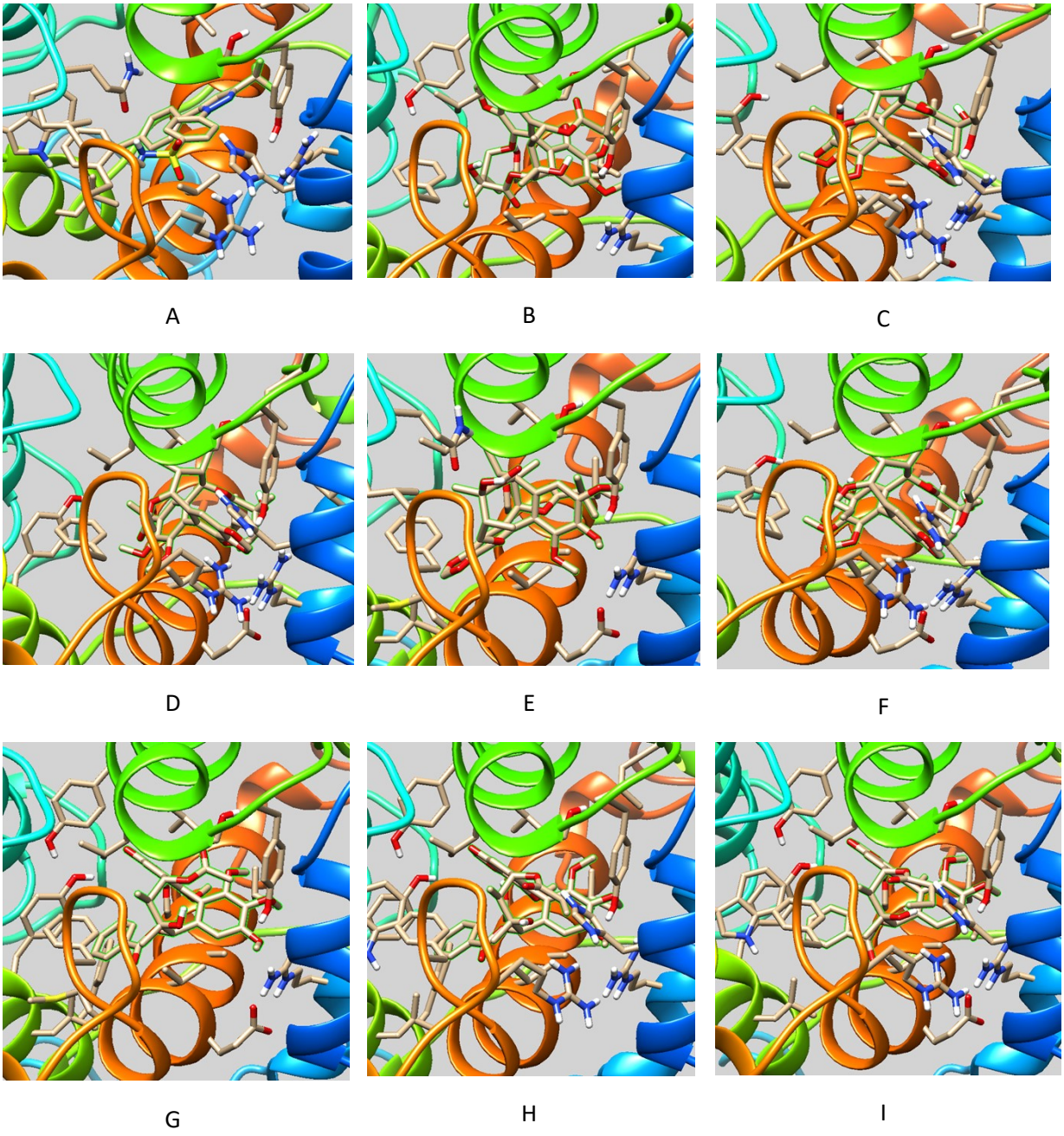

Figure S53. Docking pose of positive drug celecoxib (A) and compounds **1-8** (B-I) on COX-2

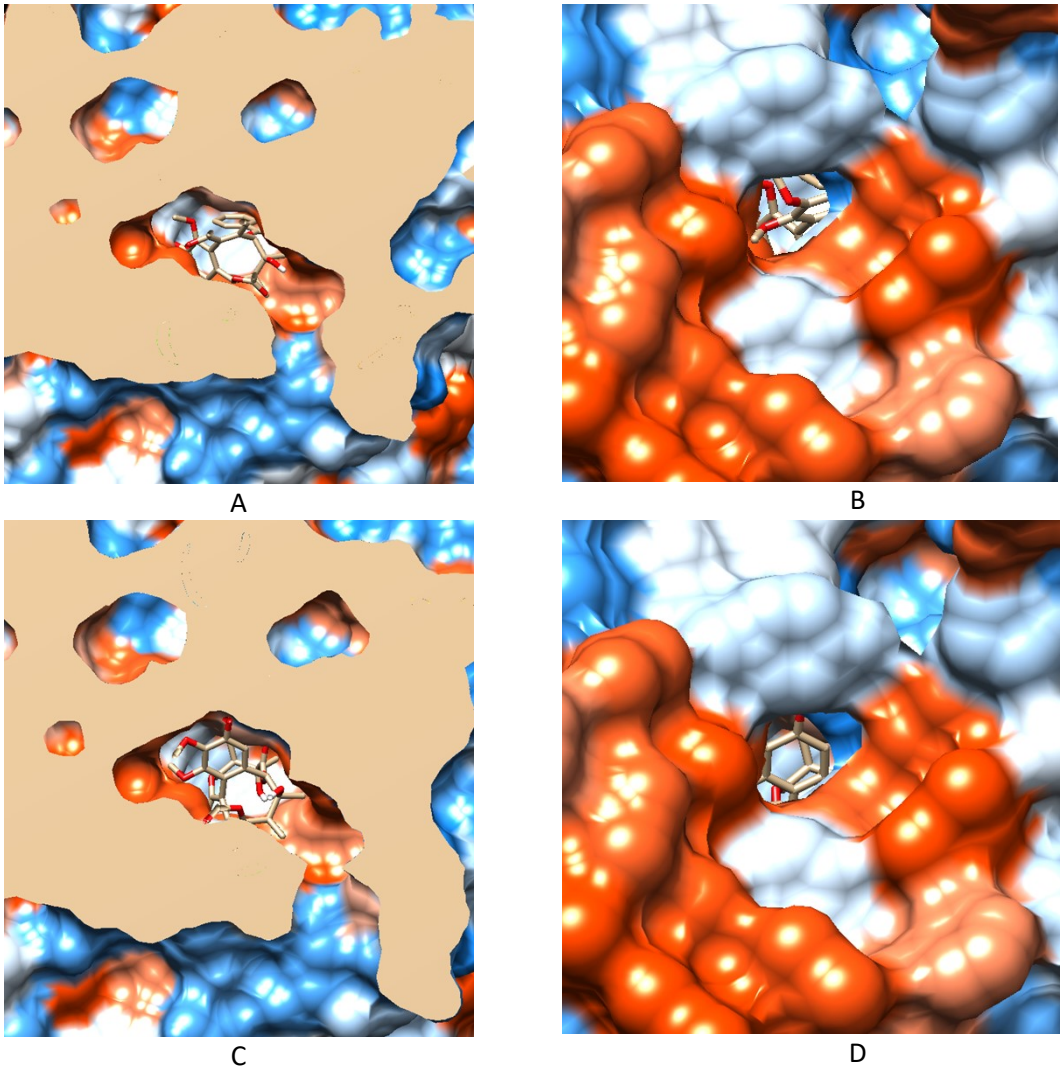

Figure S54. Simulation of compounds **7** (A: inside-pocket view, and B: overview) and **1** (C: inside-pocket view, and D: overview) at binding pocket of COX-2

Nitric oxide assay

Nitric oxide assay was performed as previously described.[1,2] In brief, RAW 264.7 cells were cultured in DMEM containing L-glutamine (2 mM), HEPES (10 mM), sodium pyruvate (1 mM), and fetal bovine serum (10%). The cells (2×10^5 cells/well) were incubated in humidified atmosphere (95% air and 5% CO_2) at 37°C. After 24h incubation, each well was added by compounds (0.4-100 μM) or vehicle and followed by LPS (1μg/mL) in the next 2h. The cells were then incubated for additional 24h. After that, cell viability was then measured by MTT assay and amount of NO production in cell medium was determined by Griess reaction. Cultural medium (100 μL) was mixed with equal volume of Griess reagent and incubated in room temperature for 10 minutes. Absorbance was measured at 540 nm on a microplate reader. Nitrite concentration as an indicator of NO production was determined using a standard curve which was built by $NaNO_2$ serial diluted solutions. Experiments were performed in triplicate. IC_{50} values were generated by TableCurve 2Dv4 software.

Reference

1. Tham PT, Chinh PT, Thang DX, et al. New sesquiterpene and flavone arabinofuranoside derivative from the leaves of Fissistigma bicolor. *Natural Product Research*. 2021:10.1080/14786419.2021.1960330. doi:10.1080/14786419.2021.1960330
2. Cheenpracha S, Park EJ, Rostama B, Pezzuto JM, Chang LC. Inhibition of nitric oxide (NO) production in lipopolysaccharide (LPS)-activated murine macrophage RAW 264.7 cells by the norsesterterpene peroxide, epimuqubilin A. *Mar Drugs*. 2010;8(3):429-37. doi:10.3390/md8030429